Targeting the secreted RGDKGE collagen fragment reduces PD-L1 by a proteasome-dependent mechanism and inhibits tumor growth

JENNIFER M. CARON[1], XIANGHUA HAN[1], CHRISTINE W. LARY[1], PRADEEP SATHYANARAYANA[1], SCOT C. REMICK[1], MARC S. ERNSTOFF[2], MEENHARD HERLYN[3] and PETER C. BROOKS[1]

[1]MaineHealth Institute for Research, Center for Molecular Medicine, Scarborough, ME 04074; [2]Division of Cancer Treatment and Diagnosis, Developmental Therapeutics Program, National Cancer Institute, Bethesda, MD 20892; [3]Wistar Institute, Philadelphia, PA 19104, USA

Received August 19, 2022; Accepted November 16, 2022

DOI: 10.3892/or.2023.8481

Abstract. Structural alterations of collagen impact signaling that helps control tumor progression and the responses to therapeutic intervention. Integrins represent a class of receptors that include members that mediate collagen signaling. However, a strategy of directly targeting integrins to control tumor growth has demonstrated limited activity in the clinical setting. New molecular understanding of integrins have revealed that these receptors can regulate both pro- and anti-tumorigenic functions in a cell type-dependent manner. Therefore, designing strategies that block pro-tumorigenic signaling, without impeding anti-tumorigenic functions, may lead to development of more effective therapies. In the present study, evidence was provided for a novel signaling cascade in which β3-integrin-mediated binding to a secreted RGDKGE-containing collagen fragment stimulates an autocrine-like signaling pathway that differentially governs the activity of both YAP and (protein kinase-A) PKA, ultimately leading to alterations in the levels of immune checkpoint molecule PD-L1 by a proteasome dependent mechanism. Selectively targeting this collagen fragment, reduced nuclear YAP levels, and enhanced PKA and proteasome activity, while also exhibiting significant antitumor activity *in vivo*. The present findings not only provided new mechanistic insight into a previously unknown autocrine-like signaling pathway that may provide tumor cells with the ability to regulate PD-L1, but our findings may also help in the development of more effective strategies to control pro-tumorigenic β3-integrin signaling without disrupting its tumor suppressive functions in other cellular compartments.

Correspondence to: Dr Peter C. Brooks, MaineHealth Institute for Research, Center for Molecular Medicine, 81 Research Drive, Scarborough, ME 04074, USA
E-mail: peter.c.brooks@mainehealth.org

Key words: extracellular matrix, stroma, collagen, integrin αvβ3, programmed death-ligand 1, YAP, protein kinase-A

Introduction

The interconnected network of extracellular matrix (ECM) proteins that help comprise the non-cellular stroma, not only provides a mechanical scaffold for cells and tissues, but can also help facilitate the ability of cells to fine tune their capacity to sense and respond to a variety of soluble external cues (1-3). The remarkable diversity of signaling cascades regulated by the ECM suggests that discrete receptor-mediated contact sites between cells and ECM proteins may function as signaling hubs that helps integrate the transfer of both solid-phase and soluble information from outside the cell to the inside (3,4). These functional signaling hubs may provide cells with the needed signaling flexibility to survive and grow in diverse tissue microenvironments (1-4).

The collagen family of molecules is a large group of triple helical matrix proteins that represent a major component of the ECM (3,5). A specific subset of the integrin family of ECM receptors are known to bind to discrete regions of intact triple helical collagen and facilitate signaling (3,6,7). Evidence indicated that while the intact triple helical conformation of collagen can stimulate signaling cascades predominately through β1-integrins, cryptic collagen elements exposed following structural remodeling can be recognized by a different subset of integrins including αvβ3, which may in turn play roles in governing cellular processes during pathological events (3,4). These cryptic collagen elements may be defined as either conformationally altered regions that are exposed within the immobilized collagen fibers, or they may be released as soluble peptide fragments (3,4). The functional importance of these cryptic elements in biological processes are beginning to emerge (3,4).

While proteolytic cleavage of pre-existing collagen allows structural remodeling of the local ECM to help create less restrictive physical barriers for migration and invasion, less is known concerning whether soluble collagen fragments bind to cell surface receptors and stimulate signaling cascades that potentiate tumor growth *in vivo*. To this end, estimates suggested that up to 20% of newly synthesized collagen can be degraded intracellularly (8), however, little is known concerning

whether these degraded collagen fragments are released from the cell and play a functional role in regulating tumor growth. Previously, an endogenously generated small bioactive collagen fragment that can be secreted by M2-like macrophages was identified (9). This 16 kDa RGDKGE-containing collagen fragment binds to and activates integrin αvβ3 expressed on vascular endothelial cells leading to enhanced nuclear accumulation of the Yes-associated protein (YAP) (9). Recently, it was also demonstrated by the authors that ovarian carcinoma cell interactions with this collagen fragment suppressed phosphorylation of the hippo effector kinase LATS1, and reduced the inhibitory phosphorylation of YAP which ultimately led to its nuclear accumulation (10). Selectively targeting this collagen fragment in ovarian carcinoma cells inhibited YAP nuclear accumulation and suppressed tumor growth *in vivo* (10).

Among the numerous factors considered to be controlled by YAP, is the immune checkpoint molecule programed death ligand-1 (PD-L1), which is expressed in a number of cell types (11-13). While the levels of soluble collagen peptides have been correlated with resistance to immune checkpoint inhibitors in humans (14,15), it is not known whether these collagen peptides play a functional role in immune suppression or directly regulate the levels of immune checkpoint molecules. Given the importance of targeting the PD-1/PD-L1 pathway to control tumor growth (16-18), obtaining a more in-depth understanding of the different mechanisms by which the levels of PD-L1 is regulated is of particular importance. Among the most well-studied mechanisms by which the levels of PD-L1 can be controlled include transcription, translation, post-translational modifications and protein stability (19-21). Studies have shown that PD-L1 can be regulated by molecules such as growth factors and cytokines including EGF, TGFβ, IL-6 and INF-γ to name just a few (19-21). Signaling stimulated through binding of these factors to their respective cell surface receptors leads to the activation of numerous pathways such as MAP/Erk, PI3K/Akt, and JAK/Stat cascades that can ultimately contribute to the differential control of PD-L1 (19-21). In addition, the levels of PD-L1 can also be controlled by alterations of protein stability through mechanism associated with glycosylation, lysosomal-mediated degradation, ER-associated degradation (ERAD) and proteasomal-mediated degradation (21-26). New evidence is now emerging that in addition to growth factor and cytokine receptor signaling, integrin receptors may also play a role in regulating PD-L1. In fact, integrins such as α2β1 and αvβ3 have been suggested to contribute to the regulation of this important immune checkpoint molecule (27-29).

In the present study, evidence was provided for the first time for a previously unappreciated signaling cascade in which β3-integrin mediated cellular interaction with the secreted RGDKGE-containing collagen fragment stimulates an autocrine-like signaling pathway that helps control PD-L1 by a proteasome dependent mechanism. Inhibiting this novel autocrine-like signaling cascade led to enhanced (protein kinase-A) PKA activity and reduced PD-L1 levels by a proteasome-dependent process. These findings are consistent with the concept that certain tumor cells have the capacity to regulate β3 integrin signaling in an autocrine-like manner by binding to this secreted soluble fragment of collagen. This autocrine-like signaling cascade may provide tumor cells with the ability to regulate PD-L1 stability by controlling PKA, YAP and proteasome function. Selectively targeting the secreted RGDKGE-containing collagen fragment inhibited tumor growth *in vivo*. Taken together, our new findings may help in establishing a novel strategy to control tumor growth by selectively disrupting an autocrine-like signaling pathway that regulates proteasome dependent control of PD-L1 levels.

Materials and methods

Cells and cell culture. B16F10 murine melanoma cells, 4T1 murine mammary carcinoma cells, HUVEC human endothelial cells, RAW264.7 murine macrophages, YUMM1.7 murine melanoma cells, A375 human melanoma cells, C32 human melanoma cells and murine Lewis Lung Carcinoma (LLC) cells designated LL/2 (LLC1) were obtained from the American Type Culture Collection (ATCC; cat. no. CRL-1642). Human Dermal Fibroblast (HDF) were obtained from ScienCell Research Laboratories, Inc. and cultured in 2% FBS in growth medium supplemented with Fibroblast Growth Supplements from ScienCell Research Laboratories, Inc. YUMM1.7 cells were cultured in DMEM F-12 medium in presence of 10% FBS, 1% NEAA and 1% Pen-Strep. 4T1 cells were cultured in RPMI-1640 medium in the presence of 5% FBS, 1% Pen-Strep and 1% sodium pyruvate. HUVECs were cultured in VCBM media plus Endothelial Cell Growth Kit. B16F10, RAW264.7, C32, A375 and LLC cells were cultured in DMEM plus 10% FBS 1.0% Pen-Strep and 1.0% sodium pyruvate. Human primary melanocytes were obtained from ScienCell Research Laboratories, Inc. and cultured in Melanocyte Media containing 0.5% FBS and Melanocyte Growth Supplement.

Animals. C57BL/6J (4-11 mice per experiment, 6-8 weeks old and 18-20 g) and Balb/CJ female mice (7 mice per experiment; 6-8 weeks old; weight 18-20 g) were obtained from the Jackson Laboratory (Bar Harbor, ME). Mice were housed in MaineHealth Institute for Research pathogen-free air barrier facility, which has a temperature range from 20-24˚C, a humidity range from 30-70% and a light/dark cycle of 14/10 h, respectively. All animal had access to food and water continuously, with no restrictions, and all handling and procedures were approved by the Maine Medical Center Institutional Animal Care and Use Committee (Scarborough, USA) under approved IACUC protocol number 2206.

Reagents, chemicals and antibodies. Bovine serum albumin (BSA), Proteasome 20S activity assay kit, MG132 proteasome inhibitor, Cathepsin inhibitor-I, DMSO and crystal violet were obtained from MilliporeSigma. Anti-YAP1 (cat. no. 14074), anti-integrin β3 (cat. no. 4702s), anti-β-tubulin (cat. no. 2145s), anti-actin (cat. no. 4907s) and anti-TATA-binding protein (TBP) (cat. no. 44059s) antibodies were all obtained from Cell Signaling Technology, Inc. Anti-PD-L1 antibody (cat. no. ab26974), the PKA kinase activity assay kit and PKA inhibitor KT5720 were all obtained from Abcam. Brefeldin-A and Super Signal Pico Plus were obtained from Thermo Fisher Scientific, Inc. Mab XL313 (cat. no. BE0324) and non-specific control antibody (cat. no. BP0083) was obtained from Bio-X Cell. P2 peptide (CQGPRGDKGEC) and control peptide CP (CQGPGGAAGGC) were from QED Bioscience. Alexa 594

labeled secondary antibody (cat. no. A11005) was from Thermo Fisher Scientific, Inc. The PKA inhibitor H89 was obtained from Selleck Chemicals. Function blocking β3 antibody (cat. no. 104310) was obtained from BioLegend, Inc. Mouse PD-L1 specific short hairpin (sh)RNAs, Coll-1α2 chain shRNAs and control non-targeting shRNAs were obtained from OriGene Technologies, Inc.

Cytotoxicity and cell growth assays. Sub-confluent B16F10 melanoma cells were washed and then resuspended in serum-free medium (DMEM) in the presence of non-specific control antibody or anti-XL313 Mab (100 μg/ml) for 1 h. Next cells were spun down and resuspended in 2.5% growth medium in the presence of non-specific control or anti-XL313 Mab (100 μg/ml) and added ($2x10^3$/well) to 96 well culture plates and allowed to proliferate for 24 h. Cell growth was quantified using Cell Proliferation Kit I (MTT) according to the manufacturer's instructions (MilliporeSigma), with formazan solubilized with 10% SDS and 0.01 M HCL solution provided with the kit. The absorbance was measured at a wavelength of 600 nm. For cytotoxicity assays, sub-confluent B16F10 cells were washed and resuspended in serum-free medium (DMEM) in suspension for 1 h in the presence of non-specific control antibody or anti-XL313 Mab (100 μg/ml). Next cells were spun down and resuspended in 1.0% serum containing medium containing 1 mM $MgCl_2$, 0.2 mM $MnCl_2$ in the presence of non-specific control or anti-XL313 Mab (100 μg/ml) and added ($2x10^3$/well) to 96 well culture plates and allowed to incubate for 24 h. Cell cytotoxicity was quantified using CytoTox 96 Non-radioactive cytotoxicity assay kit according to manufactures instructions (Promega Corporation). Cell growth and cytotoxicity was quantified from triplicate wells and assays carried out 3 independent times.

Western blot analysis. To determine if tumor cells could express the RGDKGE-containing collagen fragment, cell lysates from growing conditions and 24 h serum-free conditioned medium (CM) were collected from equal number of B16F10, C32, YUMM1.7, A375, 4T1, LLC, Raw 264.7, HUVEC, human melanocytes and HDFs. B16F10 cells ($0.5x10^6$) were serum-starved for 1 h in suspension at 37˚C. Next, cells were resuspended in 500 μl of serum-free media and incubated over a time course (0-180 min). CM and lysates were prepared at 0, 15, 60 and 180 min. To confirm that the RGDKGE containing collagen fragment was secreted, B16F10, YUMM1.7, and C32 cells were serum-starved for 1 h in suspension at 37˚C with Brefeldin-A (10 μM) or equivalent control. Next, cells were resuspended in serum-free DMEM with Brefeldin-A (10 μM) or control (methanol) for 15 min or 1 h and lysate and CM were prepared. In experiments to study the impact of cathepsin on the expression of the low molecular weight RGDKGE containing collagen fragment, sub-confluent cultures of cells were serum-starved in suspension for 1 h at 37˚C in the presence of 25 μM of Cathepsin inhibitor or control. Next, cells were resuspended in serum-free DMEM media containing cathepsin inhibitor (25 μM) or control for 3 h and lysates were prepared.

In experiments to study the mechanism by which Mab XL313 may regulate PD-L1, cells were serum-starved in suspension for 1 h at 37˚C with 10 μM MG132, 10 μM H89, 5 μM KT5720, or the equivalent control. Subsequently, cells were resuspended in serum-free DMEM with the indicated inhibitors in the presence of Mab XL313 or control antibody (100 μg/ml) for 15 min or 1 h and cell lysates were prepared.

To examine the effects of Mab XL313 on PD-L1 levels, cells from sub-confluent cultures were serum-starved in suspension for 1 h at 37˚C, then resuspended in serum-free DMEM media containing Mab XL313 or control antibody (100 μg/ml) for 15 min or 1 h and cell lysates were prepared. To examine whether RGDKGE-containing collagen fragment could counteract the effects of Brefeldin-A on PD-L1, B16F10 cells were serum-starved in suspension for 1 h with Brefeldin-A (10 μM) or control. Next, cells were resuspended in the presence of Brefeldin-A (10 μM) or control along with P2 or CP (100 ng/ml) for 15 min and lysates were then prepared. All cells were lysed in RIPA lysis buffer with 1X protease inhibitor cocktail, 2 mM of PMSF, 1 mM of sodium orthovanadate (Santa Cruz Biotechnology, Inc.). Equal amounts of cell lysates (5-30 μg per lane), determined by BCA assay, were separated by SDS PAGE (using 10 or 15% polyacrylamide gels). Membranes (0.45-μM nitrocellulose) were blocked with 10% milk-TBST for 1 h at room temperature. Primary antibodies were diluted in 5% BSA-TBST. Primary antibodies were incubated (Mab XL313, 5 μg/ml), anti-PD-L1 (2 μg/ml), anti YAP (1:1,000) anti-Tubulin (1:5,000), anti-Actin (1:1,000) with membranes overnight at 4˚C. Secondary antibodies (anti-mouse HRP-labeled, cat. no. W4021; and anti-rabbit HRP-labeled, cat. no. W4011; both diluted at 1:10,000 from Promega Corporation) were diluted in 5% milk-TBST and incubated for 1 h at room temperature. Western blots were performed at least 3 to 4 times and visualized by chemiluminescence detection using Super Signal Pico Plus obtained from Thermo Fisher Scientific, Inc. Quantification of the mean relative changes in proteins was carried out using ImageJ software (version 5.0; National Institutes of Health).

Preparation of tissue lysates. Female C57BL/6J or Balb/CJ mice (6-8 weeks old) were injected with B16F10 or 4T1 cells, respectively. Individual tumors (n=4) were harvested and snap frozen on dry ice and ground in a cold mortar. Ground up tissues from individual tumors were mixed with RIPA lysis buffer, and whole tumor tissue lysates were generated for western blot analysis. Fully de-identified snap frozen human melanoma biopsy tissues were obtained from MaineHealth Institute for Research Bio Bank and tissue lysates were generated as aforementioned.

Cell line generation. Cd274 mouse shRNA plasmid (TL503436) specific for Pd-l1 or scrambled non-targeting (NT) shRNA plasmid (TL30021) containing the backbone cassette in PGFP-C-shLenti shRNA vectors (2.5 μg of plasmids per 6-well plates) were transfected to B16F10 cells at 37˚C with TurboFectin™ 8.0 transfection reagent (cat. no. TF81001) from OriGene Technologies, Inc. according to the manufacturer's instructions. After 24 h of transfection, the cells were selected with 3 μg/ml of puromycin containing growth medium to generate stably expressing shRNA cell lines. The effective targeting sequence of Pd-l1 gene is 5'-GTG GTGGAGTATGGCAGCAACGTCACGAT-3'. The Col-1α2 shRNA plasmid (TL500407) or scrambled negative control

non-targeting shRNA plasmid (TR30021) containing the backbone cassette in PGFP-C-shLenti shRNA vectors, were obtained from OriGene Technologies, Inc. B16F10 cells were transfected with lipofectamine 3000 transfection kit (L3000) from Invitrogen by Thermo Fisher Scientific, Inc. After 24 h of transfection, the cells were selected with 3 μg/ml of puromycin containing growth medium. The effective targeting sequence of Coll-1 α2 gene is 5'-AGTGGTCCTCAAGGC ATCCGAGGTGACAA-3'. Next, the same number of actively growing cells were seeded for determining knock down efficiency by reverse transcription-quantitative (RT-q)PCR and the RGDKGE-containing collagen fragment expression by western blotting. The murine RT-qPCR primers specific for collagen-1 α2 chain were forward, 5'-CTAGCCAACCGT GCTTCTCA-3' and reverse, 5' TCTCCTCATCCAGGTACG CA-3'. For the housekeeping gene of mouse Cyclophilin, the primers were forward, 5'-CCACCGTGTTCTTCGACAT-3' and reverse, 5'-CAGTGCTCAGAGCTCGAAAG-3'. RT-qPCR assays were repeated at least 3 times.

Nuclear protein extraction. To examine the effects of blocking cellular interactions with the secreted RGDKGE-containing collagen fragment on nuclear accumulation of YAP, sub-confluent B16F10 cells were washed and serum-starved for 1 h in suspension at 37˚C and cells were then resuspended in media containing Mab XL313 or nonspecific control antibody (100 μg/ml) for 15 min. The nuclear and cytoplasmic proteins were extracted using NE-PER nuclear and cytoplasmic extraction reagents from Thermo Fisher Scientific, Inc. according to the manufacturer's instructions. The nuclear extractions were examined by western blot analysis with anti-YAP or anti-TBP (TATA binding protein) antibody.

RNA isolation, cDNA synthesis and RT-qPCR. Sub-confluent B16F10 cells were washed and serum-starved in suspension for 1 h at 37˚C. Next, cells were resuspended in media containing Mab XL313 or control antibody (100 μg/ml). To examine the effects of Mab XL313 on PD-L1 levels, cells were lysed after incubation over a time course of 15 min, 1 and 3 h using RNA isolation lysis buffer. RNA was isolated by using RNase plus mini kit from Qiagen following the manufacturer's protocol. Total RNA (1.0 μg) was synthesized with iScript cDNA synthesis kit from Bio-Rad Laboratories, Inc according to the manufacturer's instruction. Equivalent amount of cDNA was used for RT-qPCR, and the murine RT-qPCR primers used for mouse *Pd-l1* were forward, 5'-TGCGGACTACAA GCGAATCACG-3' and reverse, 5'-CTCAGCTTCTGGATA ACCCTCG-3' and for the housekeeping gene mouse b2m, the primers were forward, 5'-CTGACCGGCCTGTATGCTAT-3' and reverse, 5'-CCGTTCTTCAGCATTTGGAT-3'. RT-qPCR assays were repeated 5 times. The expression of Pd-l1 genes was examined by RT-qPCR using Bio-Rad CFX connect real time systems with a SYBR green-based 3 step amplification protocol. The reaction was set up by incubation at 95˚C for 3 min for initial denaturation, followed by 45 cycles of denaturation, annealing, and extension steps (95˚C for 10 sec, 57˚C for 30 sec and 72˚C for 30 sec), with data collection at each annealing step. To ensure the specificity of the amplifications, each amplification reaction was followed by a melting phase, according to the default settings of the CFX connect instrument (from 65 to 95˚C), and each melting curve was assessed for the presence of a single peak. The transcript level of the Pd-l1 gene was normalized to the transcript level of house-keeping gene b2m. The method of quantification used was $2^{-\Delta\Delta Cq}$ (30).

Immunofluorescence staining. Sub-confluent B16F10 melanoma cells were harvested from culture and washed. B16F10 cells were serum-starved for 1 h in suspension and plated on 10% serum-coated slides and allowed to attach for 1 h. Cells were washed and fixed with 50% acetone and 50% methanol for 10 min. Next cells were washed and incubated for 1 h at room temperature with anti-PD-L1 antibody (cat. no. NBP1-76769; Novus Biologicals, LLC) (10 μg/ml diluted in 1.0% BSA in PBS). Next, cells were washed 3 times in PBS and incubated for 30 min with both alexa-594 secondary antibody (cat. no. A11005) (1:5,000) and DAPI (1:3,000) from Thermo Fisher Scientific, Inc. Finally, cells were washed and mounted for analysis.

Proteasome 20S activity assay. To examine whether the effects of Mab XL313 on PD-L1 were due to proteasome-mediated degradation, a proteasome activity assay kit from MilliporeSigma was used. Briefly, B16F10, B16F10-YAP-K/D (Yap knock down), and B16F10-NT (non-targeting vector) cells were serum-starved for 1 h at 37˚C in suspension. Afterwards, cells were resuspended in serum-free DMEM containing Mab XL313, non-specific control IgG (100 μg/ml) or anti-β3 antibody (50 μg/ml) for 15 min. For stimulation with control peptide CP or collagen peptide P2, cells were stimulated with peptides (100 ng/ml) for 5 min. Next, cells were spun down, and media was replaced with 300 μl of Proteasome Loading Solution and 100 μl was added to a 96 well flat bottom black plate (in triplicate) according to the manufacturer's protocol. The plate was incubated at 37˚C for 1 h and then the fluorescence intensity was measured using an excitation wavelength at 490 nm and emission wavelength at 525 nm. Proteasome activity assays were performed in triplicate 3 to 4 times.

PKA activity assay. To examine whether the Mab XL313 or the collagen peptide P2 impacts PKA activity, a PKA activity assay obtained from Abcam was performed using cell lysates. Briefly, B16F10, B16F10-NT and B16F10-YAP-K/D cell lysates were prepared by serum-starving cells in suspension for 1 h at 37˚C. Next, cells were resuspended in serum-free DMEM containing Mab XL313, non-specific control IgG or function blocking anti-β3 antibody for 15 min. In similar studies, B16F10 cells were serum-starved in suspension for 1 h at 37˚C. Next, cells were resuspended in serum-free DMEM containing either control peptide CP (100 ng/ml) or collagen peptide P2 (100 ng/ml) for 15 min. Cells were then lysed in RIPA lysis buffer with 1X protease inhibitor cocktail, 2 mM of PMSF, 1 mM of sodium orthovanadate and stored at -80˚C. The PKA activity assay was performed according to the manufacturer's instructions. PKA activity assays were performed in triplicate 3 to 4 times.

Cell binding assays. A total of 48 well non-tissue culture plates were coated with 100 μg/ml of control peptide (CP) or RGDKGE-containing peptide (P2). Tumor cells were suspended in adhesion buffer (DMEM) containing 1 mM

$MgCl_2$, 0.2 mM $MnCl_2$ and 0.5% BSA, and $1x10^5$ cells were added to the wells in the presence of 100 μg/ml of Mab XL313, anti-β3 integrin antibody, anti-β1 integrin antibody or non-specific control IgG and allowed to bind for 10-20 min at 37˚C. Non-attached cells were removed and attached cells were stained with crystal violet as previously described (10,31). Cell binding was quantified by measuring the optical density of eluted dye as previously described (10,31). Cell binding assays were performed at least 3 times with triplicate wells per condition.

Viral vectors for cell line generation. Lentiviral vectors (pLKO.1 based) encoding short hairpin RNAs (shRNAs) specific for *YAP* or a control non-targeting construct developed by the RNAi Consortium were obtained from GE Healthcare Life Science. The effective targeting sequence of *YAP* gene was 5'-TTCTTTATCTAGCTTGGTGGC-3'. Lentivirus was packaged in the recombinant viral vector core facility at MaineHealth Institute for Research. Multiplicity of infection (MOI) was 1. B16F10 cells were transduced with shRNA overnight in a viral culture room incubator. The next day, transduced cells were washed twice with PBS and fresh growth medium was added in the presence of 3 μg/ml of puromycin (Invitrogen; Thermo Fisher Scientific, Inc.) and brought to the lab cell culture incubator. After 7-10 days of selection, the established stable cell pool was used to determine the knockdown efficiency by western blot. Once knockdown efficiency was confirmed, transduced cells were used for further experiments within approximately 2 to 3 weeks. Cells were periodically tested prior to carrying out experiments to confirm knockdown efficiency by western blot.

Tumor growth assays. Tumor growth assays were performed as previously described (10,30). Briefly, mice were injected subcutaneously with either $3.5x10^5$ B16F10 cells, non-target B16F10 cells, $3.5x10^6$ PD-L1 knock-down B16F10 (N=8-10 C57BL/6 mice per condition) or $3x10^5$ 4T1 mammary carcinoma cells resuspended in 100 μl of sterile PBS. Mice were allowed to form palpable tumors for 3 or 7 days, then the mice were intraperitoneally injected with Mab XL313 or nonspecific control antibody (0-250 μg/mouse) 3X times per week for 14 or 21 days. Tumor size was measured with caliper and the tumor volume was calculated using the formula $V=L^2 x W/2$, where V=volume, L=length, W=width. All mice were euthanized by inhalant isoflurane to effect by administering isoflurane from a 100% stock solution as a vapor in a closed chamber until lack of breathing and heartbeat was observed, which was followed by cervical dislocation. Death was verified by lack of breathing and lack of heartbeat determined by palpation in accordance with MaineHealth IACUC approved protocol number 2206.

Statistical analysis. Statistical analysis was performed using the Prism/Graph Pad (version 6; GraphPad Software, Inc.) statistical program for Macintosh computers. Data were analyzed for statistical significance using unpaired Student's t-test with comparison to the control group, performed separately at each time point. For experiments in which there were more than two groups, we performed a one-way ANOVA and then used a Dunnett's multiple comparison test to adjust for comparison of each level to the control group. $P<0.05$ was considered to indicate a statistically significant difference.

Results

Detection of the RGDKGE-containing collagen fragment in malignant tumor cells and effects of targeting it on tumor growth in vivo. While it is well-accepted that cellular interactions with triple helical collagen can regulate the behavior of distinct tumors (31-34), less is known concerning the impact of endogenously secreted soluble collagen fragments have on malignant cells. While stromal cells such as fibroblasts represent a major source of collagen, other cells types within tumor lesions also express collagen, including alternatively activated M2-like macrophages (9,35,36). We identified a bioactive 16 kDa RGDKGE-containing collagen fragment that can be secreted from M2-like macrophages (9). To determine the expression of this collagen fragment within different tumor cells, we analyzed serum-free CM and whole cell lysates from a panel of different tumor cell lines. To facilitate these studies, Mab XL313 was used, which specifically recognizes the RGDKGE sequence within proteolyzed collagen, but does not bind to intact collagen or other RGD-containing ECM molecules (9). The low molecular weight 16 kDa RGDKGE-containing collagen fragment was detected within whole cell lysates and in serum-free CM from several tumor cell lines including B16F10 melanoma, 4T1 mammary carcinoma and LLC (Fig. 1A). By contrast, while this low molecular weight collagen fragment was detected in RAW 264.7 macrophages, it was not detected in normal human melanocytes, endothelial cells (HUVEC) or HDF (Fig. 1B). The RGDKGE-containing collagen fragment was also detected within both whole cell lysates and serum-free CM in additional tumor cell lines including C32 and YUMM1.7 cells, while A375 cells expressed minimal if any detectable levels (Fig. 1C). In addition, the RGDKGE-containing collagen fragment was also detected in whole tissue lysates of 4T1 mammary carcinomas and B16F10 melanomas growing *in vivo* (Fig. 1D and E), as well as in malignant human melanoma biopsies (Fig. 1F). Collectively, these data indicated that the RGDKGE-containing collagen fragment can be differentially generated by several different tumor cell lines and malignant human melanomas.

Taking into consideration previous studies by the authors (9,10), it was sought to confirm that different tumor cell types also have the capacity to directly interact with the RGDKGE-containing collagen fragment. Similar to previous studies (9,10), a synthetic RGDKGE-containing collagen fragment termed P2, which is specifically recognized by anti-XL313 Mab (9), can bind to a variety of distinct tumor cell lines, including 4T1 mammary carcinomas and a number of melanoma cell lines including B16F10, C32 and YUMM1.7 (Fig. S1A-D). To confirm the function blocking activity of anti-XL313 Mab, the ability of Mab XL313 to block tumor cell interaction with the RGDKGE-containing collagen fragment P2 was examined. As revealed in Fig. 1G and H anti-XL313 Mab inhibited B16F10 and 4T1 tumor cell binding to this

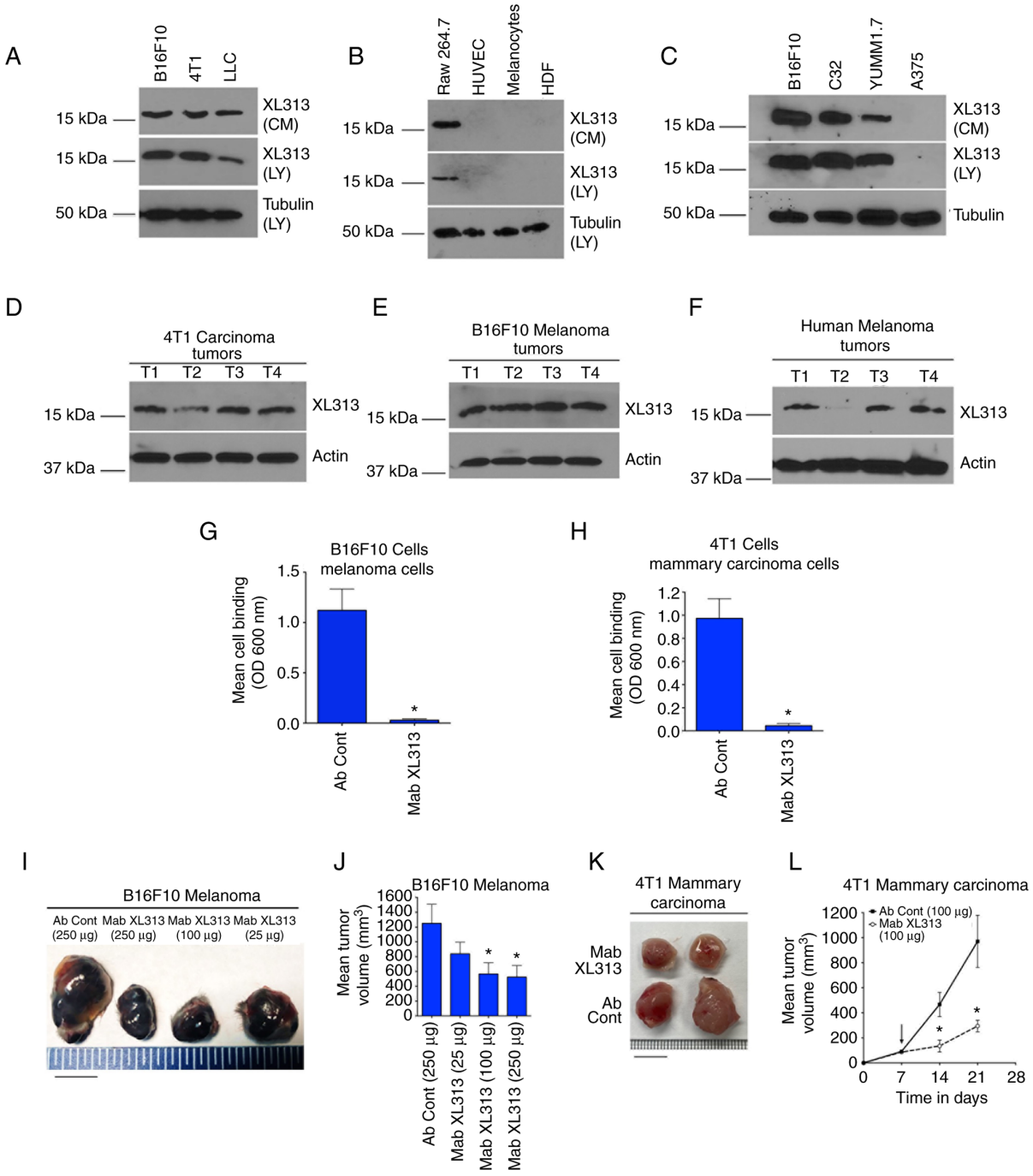

Figure 1. RGDKGE-containing collagen fragment in distinct tumor types. (A-C) Western blot analysis of LY and serum-free CM for the 16 kDa RGDKGE-containing collagen fragment or loading control tubulin in (A) B16F10 melanoma, 4T1 mammary carcinoma and LLC; in (B) macrophages (RAW 264.7), endothelial cells (HUVEC), normal human melanocytes and HDF and in (C) B16F10 melanoma, C32 melanoma, YUMM1.7 melanoma and A375 melanoma cells. (D and E) Western blot analysis of lysates from individual solid (D) 4T1 and (E) B16F10 tumors growing in mice for the 16 kDa RGDKGE-containing collagen fragment or loading control actin. (F) Western blot analysis of lysates from individual biopsies of malignant human melanoma tumors for the 16 kDa RGDKGE-containing collagen fragment or loading control actin. (G and H) Quantification of (G) B16F10 and (H) 4T1 cell binding to collagen peptide P2 in the presence of non-specific control antibody (Ab Cont) or anti-RGDKGE antibody (Mab XL313). Data bars represent the mean ± SEM cell binding from triplicate wells. (I) Example of changes in B16F10 tumor size following treatment of mice with different doses of Mab XL313 or control antibody (Ab Cont) (scale bar, 1 cm). (J) Quantification of the dose-dependent effects of anti-RGDKGE collagen fragment antibody (Mab XL313) or non-specific control antibody (Ab Cont) on the growth B16F10 tumors *in vivo*. Data bars indicate the mean ± SEM tumor volumes (n=4-6 per group). P-value represents comparison of each group to antibody control. (K) Example of changes in 4T1 tumor size following treatment of mice with Mab XL313 or control antibody (Ab Cont) (scale bar, 1 cm). (L) Quantification of the effects of anti-RGDKGE collagen fragment antibody (Mab XL313) or non-specific control antibody (Ab Cont) on the growth 4T1 tumors *in vivo*. Data bars indicate the mean ± SEM tumor volumes (n=7 per group). *P<0.05 vs. control at each time point. LY, whole cell lysates; CM, conditioned medium; LLC, Lewis Lung Carcinoma; HDF, human dermal fibroblasts; Mab, monoclonal antibody.

RGDKGE-containing collagen fragment. Similar results were observed with C32 and YUMM1.7 melanoma cells (Fig. S1E and F).

Given the expression of the RGDKGE-containing collagen fragment in tumor tissues, it was next sought to examine the therapeutic impact of selectively targeting the bioactive

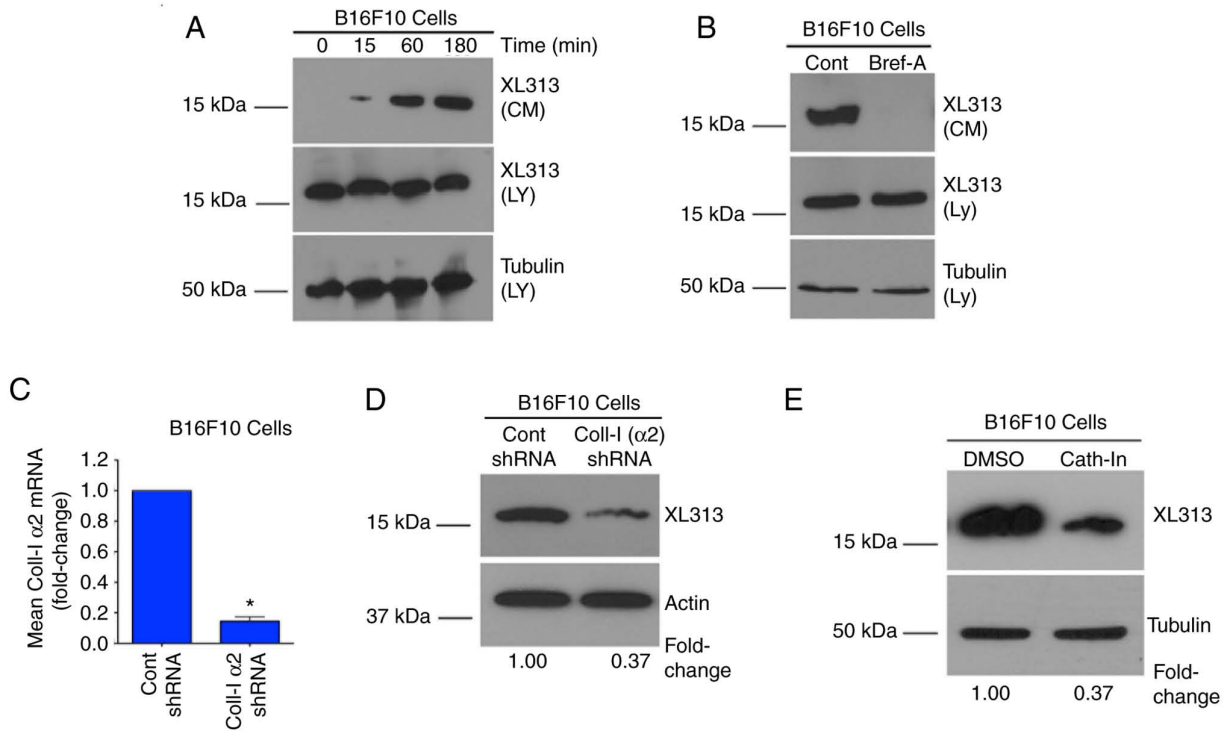

Figure 2. Secreted RGDKGE-containing collagen fragment is generated by a cathepsin-dependent process. (A) Western blot analysis of LY and serum-free CM for the 16 kDa RGDKGE-containing collagen fragment or loading control tubulin in non-attached B16F10 melanoma cells over a time course. (B) Western blot analysis of LY and serum-free CM for the 16 kDa RGDKGE-containing collagen fragment or loading control tubulin in non-attached B16F10 cells treated with Brefeldin-A. (C) Quantification of the mean ± SEM fold change in Coll-1(α2) mRNA in Coll-1 (α2) specific shRNA transfected and non-targeting control shRNA-transfected B16F10 cells. (D) Western blot analysis of whole cell lysates for the 16 kDa RGDKGE-containing collagen fragment or loading control actin in non-targeting (Cont shRNA) and Coll-1 (α2) knockdown B16F10 cells. (E) Western blot analysis of whole cell lysates for the 16 kDa RGDKGE-containing collagen fragment or loading control tubulin in non-attached B16F10 cells treated with Cath-In or control DMSO. LY, whole cell lysates; CM, conditioned medium; shRNA, shorth hairpin RNA; Cath-In, cathepsin inhibitor. *P<0.05.

RGDKGE-containing collagen fragment. To begin these studies, the dose-dependent impact of Mab XL313 on B16F10 tumors growing *in vivo* was examined. As demonstrated in Fig. 1I and J and Table SI, treatment of mice with established B16F10 tumors with Mab XL313 resulted in a dose-dependent inhibitory effect, with a significant inhibition of ~50% achieved at doses of 100 μg per each mouse 3 times per week. To confirm the antitumor activity of Mab XL313 in a second independent *in vivo* tumor model, 4T1 mammary carcinomas growing in Balb/c mice were used. As shown in Fig. 1K and L and Table SII, anti-XL313 Mab also significantly inhibited 4T1 mammary carcinoma tumor growth.

The RGDKGE-containing collagen fragment can be generated by a cathepsin-dependent process. To further study the RGDKGE-containing collagen fragment, it was chosen to focus primarily on B16F10 melanoma cells and started by examining the kinetics of the release of this collagen fragment. To facilitate these studies, B16F10 cells were serum-starved in suspension for 1 h and then washed and resuspended in serum-free medium and CM was collected over a time course of 3 h. Beginning as early as 15 min, a time-dependent increase in the accumulation of the low molecular weight 16 kDa RGDKGE collagen fragment was observed in the CM (Fig. 2A). To confirm that the collagen fragment detected within the CM was actively secreted, CM was collected from cells that were first pre-treated with the ER/Golgi inhibitor Brefeldin-A, which inhibits protein secretion. As revealed in Fig. 2B, secretion of this collagen fragment was inhibited by Brefeldin-A treatment. Similar findings were also observed with C32 and YUMM1.7 melanoma cells (Fig. S2A and B). These data are consistent with the ability of cells to secrete the soluble 16 kDa RGDKGE-containing collagen fragment by an ER/Golgi dependent mechanism.

Previous studies indicated that knocking down collagen could reduce the levels of the RGDKGE-containing collagen fragment in macrophages (9). To confirm these findings, collagen was knocked down in B16F10 cells (Fig. 2C) and the levels of the RGDKGE-containing collagen fragment were examined. As expected, knocking down the a2 chain of collagen-1 reduced the RGDKGE-containing collagen fragment (Fig. 2D). Importantly, up to 20% of newly synthesized collagen can be proteolyzed intracellularly (8). Cathepsins represent a major family of intracellular enzymes capable of cleaving collagen. Therefore, it was examined whether cathepsins played a role in the generation of the low molecular weight RGDKGE-containing collagen fragment. To test this possibility, B16F10 cells were incubated with a cell permeable cathepsin inhibitor. As anticipated, treatment of melanoma cells with the cathepsin inhibitor reduced the levels of the RGDKGE-containing collagen fragment (Fig. 2E). Similar results were also observed following treatment of C32 and YUMM1.7 melanoma cells (Fig. S2C and D). Collectively, these findings are consistent with a role for cathepsin in

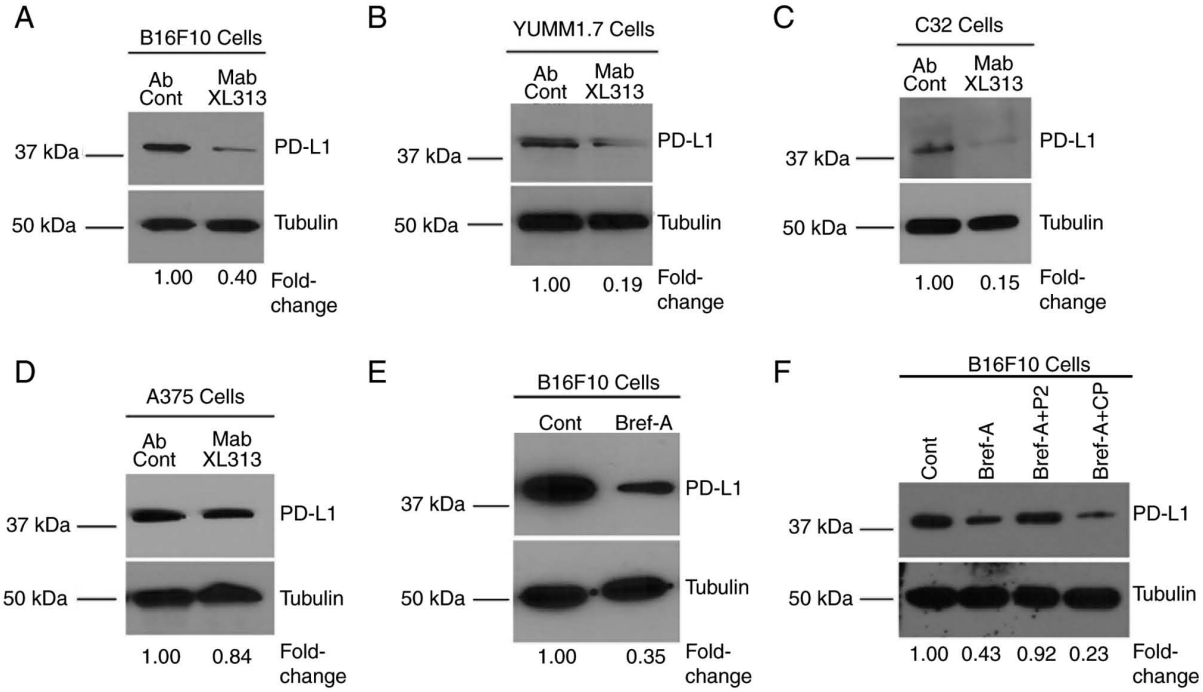

Figure 3. Selective targeting of the secreted RGDKGE-containing collagen fragment reduces PD-L1 levels in tumor cells. (A-D) Western blot analysis of whole cell lysates for PD-L1 or loading control tubulin in non-attached (A) B16F10, (B) YUMM1.7, (C) C32 and (D) A375 tumor cells treated for 1 h with anti-RGDKGE collagen fragment antibody (Mab XL313) or non-specific control (Ab Cont). (E) Western blot analysis of whole cell lysates for PD-L1 or loading control tubulin in non-attached B16F10 cells treated with vehicle (Cont) or Bref-A. (F) Western blot analysis of whole cell lysates for PD-L1 or loading control tubulin in non-attached B16F10 cells treated with vehicle (Cont), Bref-A, Bref-A plus the RGDKGE-containing collagen peptide P2 (Bref-A + P2) or Bref-A plus control peptide (Bref-A + CP). PD-L1, programmed death-ligand 1; Bref-A, Brefeldin-A.

generating the low molecular weight RGDKGE-containing collagen fragment in these cells.

Selectively targeting the secreted RGDKGE-containing collagen fragment reduces PD-L1 levels. Previous studies indicated that blocking β3 integrin-mediated interactions with the RGDKGE-containing collagen fragment inhibits YAP nuclear accumulation in endothelial cells as well as ovarian carcinoma cells (9,10). Notably, both β3 integrin and YAP have been shown to regulate the levels of the immune checkpoint molecule PD-L1 (11-13). Thus, it was sought to determine whether the secreted RGDKGE-containing collagen fragment may regulate PD-L1. To begin these studies, the expression of PD-L1 in B16F10 cells was first confirmed. Consistent with previous studies (37), B16F10 cells readily expressed PD-L1 (Fig. S3A). Next, it was confirmed that B16F10 cells use β3 integrin to bind to the RGDKGE-containing collagen fragment. As expected, B16F10 melanoma cells bind to the RGDKGE-containing collagen fragment in a β3 integrin-dependent manner as B16F10 cell interaction with P2 could be inhibited by anti-β3 integrin antibody, but not by anti-β1 integrin antibody or non-specific control antibody (Fig. S3B).

Next, it was determined whether blocking the RGDKGE-containing collagen fragment may affect PD-L1 levels. As revealed in Fig. 3A-C, targeting the secreted collagen fragment with Mab XL313 reduced PD-L1 by ~60-80% in B16F10, C32 and YUMM1.7 cells, while treatment of A375 cells, which express little if any of the RGDKGE-containing collagen fragment (Fig. 1C) had minimal impact on PD-L1 levels (Fig. 3D). Notably, PD-L1 was also reduced in cells in which the secretion of the RGDKGE collagen fragment was inhibited with Brefeldin-A (Fig. 3E), and the level of PD-L1 in Brefeldin-treated cells could be restored to near control levels by the addition of exogenous RGDKGE-containing collagen peptide P2, but not by treatment with control peptide CP (Fig. 3F). Previous studies have suggested that reduction of PD-L1 in some tumor cell lines may affect cell growth and survival (38-40). To this end, the effects of Mab XL313 on B16F10 cell cytotoxicity were first examined *in vitro*. Incubation of B16F10 cells with Mab XL313 failed to exhibit any significant effect on B16F10 cell cytotoxicity compared with non-specific control antibody (Fig. S3C). Next, the effects of anti-XL313 Mab on cell growth were examined. Incubation of B16F10 cells with Mab XL313 showed a small but significant inhibitory effect on cell growth (Fig. S3D), which was consistent with previously published results suggesting that reduction of PD-L1 may impact B16F10 tumor cell *growth in vitro* (38). Since β3 integrin can serve as a receptor for the collagen fragment, experiments were carried out to assess the effects of directly inhibiting β3 integrin may have on PD-L1. Selectively targeting β3-integrin with a function-blocking antibody also reduced the levels of PD-L1 (Fig. S3E). Collectively, these data are consistent with an autocrine-like pathway involving the secreted RGDKGE collagen fragment binding to β3-integrin that regulates the levels of PD-L1.

The ability of Mab XL313 to regulate PD-L1 in B16F10 cells depends on YAP. Given our previous findings that the RGDKGE-containing collagen fragment can regulate nuclear

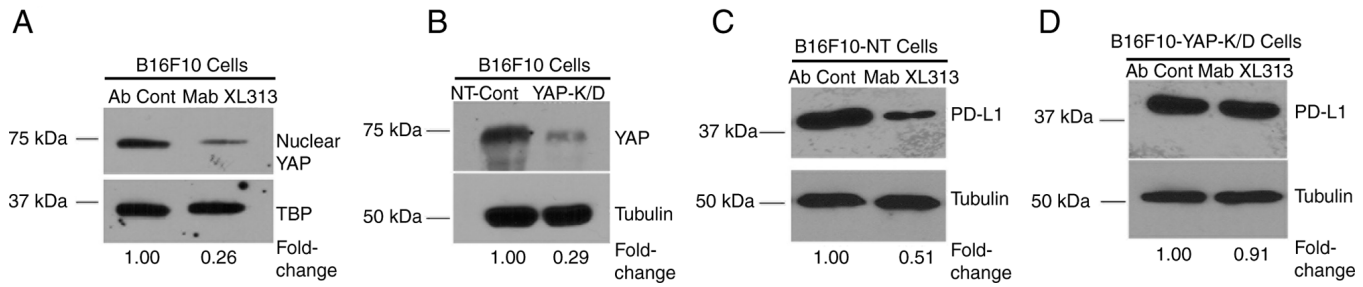

Figure 4. Reduction of PD-L1 levels in B16F10 cells by selectively targeting the RGDKGE collagen fragment depends on YAP. (A) Western blot analysis of nuclear extracts for YAP or loading control TBP in B16F10 cells treated with anti-RGDKGE collagen fragment antibody (Mab XL313) or non-specific control (Ab Cont). (B) Western blot analysis of cell whole cell lysates for YAP or loading control tubulin in control non-targeting shRNA (NT-shRNA) and *Yap*-shRNA knock down B16F10 cells. (C) Western blot analysis of whole cell lysates for PD-L1 or loading control tubulin in non-attached control transfected B16F10 cells (B16F10-NT) treated with anti-RGDKGE collagen fragment antibody (Mab XL313) or non-specific control (Ab Cont). (D) Western blot analysis of whole cell lysates for PD-L1 or loading control tubulin in non-attached *Yap*-knock down transfected B16F10 cells (B16F10-YAP/K/D) treated with anti-RGDKGE collagen fragment antibody (Mab XL313) or non-specific control (Ab Cont). PD-L1, programmed death-ligand 1; shRNA, short hairpin RNA; Mab, monoclonal antibody.

accumulation of YAP (9,10), it was assessed whether the ability of this secreted collagen fragment to control PD-L1 depends on YAP. First, it was confirmed that blocking the RGDKGE collagen fragment with Mab XL313 reduced nuclear YAP levels in B16F10 cells. As expected, treatment of B16F10 cells with anti-XL313 Mab reduced nuclear YAP levels (Fig. 4A). Next, yap gene expression was knocked down in B16F10 cells (Fig. 4B), and the ability of Mab XL313 to reduce PD-L1 was compared in either control-transfected (B16F10-NT) or in YAP knock-down cells (B16F10-YAP-K/D). While specifically targeting the RGDKGE collagen fragment with Mab XL313 reduced PD-L1 levels in control transfected cells (Fig. 4C), Mab XL313 failed to significantly alter PD-L1 levels in YAP knock-down cells (Fig. 4D). These data are consistent with a role for YAP in mediating the ability of this collagen fragment to regulate PD-L1.

Selectively targeting the RGDKGE-containing collagen fragment reduces PD-L1 levels by a proteasome-dependent mechanism. Studies have suggested that YAP can contribute to the control of PD-L1 by regulating its transcription or indirectly by regulating the expression of cytokines and growth factors known to modulate PD-L1 expression (11-13,19,20). Given that the secreted RGDKGE-containing collagen fragment can regulate PD-L1, it was sought to examine possible mechanisms to account for this effect. Given the relatively rapid change in levels of PD-L1 that can be observed within 15 min of treating cells with Mab XL313 (Fig. S4A), it appeared unlikely that this change was associated with alterations in transcription. Consistent with this notion, RT-qPCR analysis of cells treated with either control antibody or Mab XL313 for 15 min resulted in no significant change in the levels of PD-L1 mRNA (Fig. 5A). Moreover, targeting the RGDKGE-containing collagen fragment with Mab XL313 also failed to significantly affect PD-L1 mRNA at later time-points including 1 and 3 h (Fig. S4B and C), suggesting that the reduction of PD-L1 protein was not related to changes in mRNA levels.

Changes in PD-L1 protein can occur as a result of proteasome-mediated degradation (21-23). Thus, it was examined whether the ability of Mab XL313 to alter PD-L1 was associated with proteasome activity. First, the ability of the XL313 antibody to reduce PD-L1 levels was assessed in the presence or absence of the proteasome inhibitor MG132. As demonstrated in Fig. 5B, B16F10 cells that were first pre-treated with control DMSO and then treated with Mab XL313, exhibited reduced levels of PD-L1. By contrast, no significant changes in PD-L1 were detected following treatment of cells with Mab XL313 that had been pre-treated with the proteasome inhibitor MG132 (Fig. 5B). Similar results were also observed with C32 and YUMM1.7 cells (Fig. S5A and B). These observations are consistent with the possibility that this collagen fragment may affect proteasome activity. The effects on proteasome activity of Brefeldin-A, which inhibits secretion of the RGDKGE collagen fragment, were next examined. Notably, Brefeldin-A treatment of B16F10 cells significantly enhanced proteasome activity by nearly 1.7-fold compared with control treatment (Fig. 5C). Given that Brefeldin-A can inhibit secretion of this collagen fragment, the effects on proteasome activity of treating B16F10 cells with exogenously added RGDKGE-containing collagen peptide (P2) were next assessed. As revealed in Fig. 5D, treatment of cells with the RGDKGE-containing collagen peptide P2 reduced proteasome activity compared with control peptide CP. Next, it was sought to determine the effects of selectively targeting the collagen fragment or its cell surface receptor integrin β3 may have on proteasome activity. As demonstrated in Fig. 5E and F, targeting either the RGDKGE collagen fragment with Mab XL313 or its cell surface receptor with anti-β3 antibody enhanced the relative proteasome activity compared with controls. Collectively, these new findings are consistent with the notion that inhibiting the RGDKGE-containing collagen fragment controls PD-L1 levels through modulation of proteasome activity.

The ability of the RGDKGE-containing collagen fragment to control PD-L1 depends on regulation of PKA activity. Prior evidence indicated that proteasome activity can be controlled in part, by PKA (41-44). Previous studies also suggested that integrin dependent signaling may suppress PKA activity in certain cell types (45,46). These observations coupled with studies indicating cross talk signaling between PKA

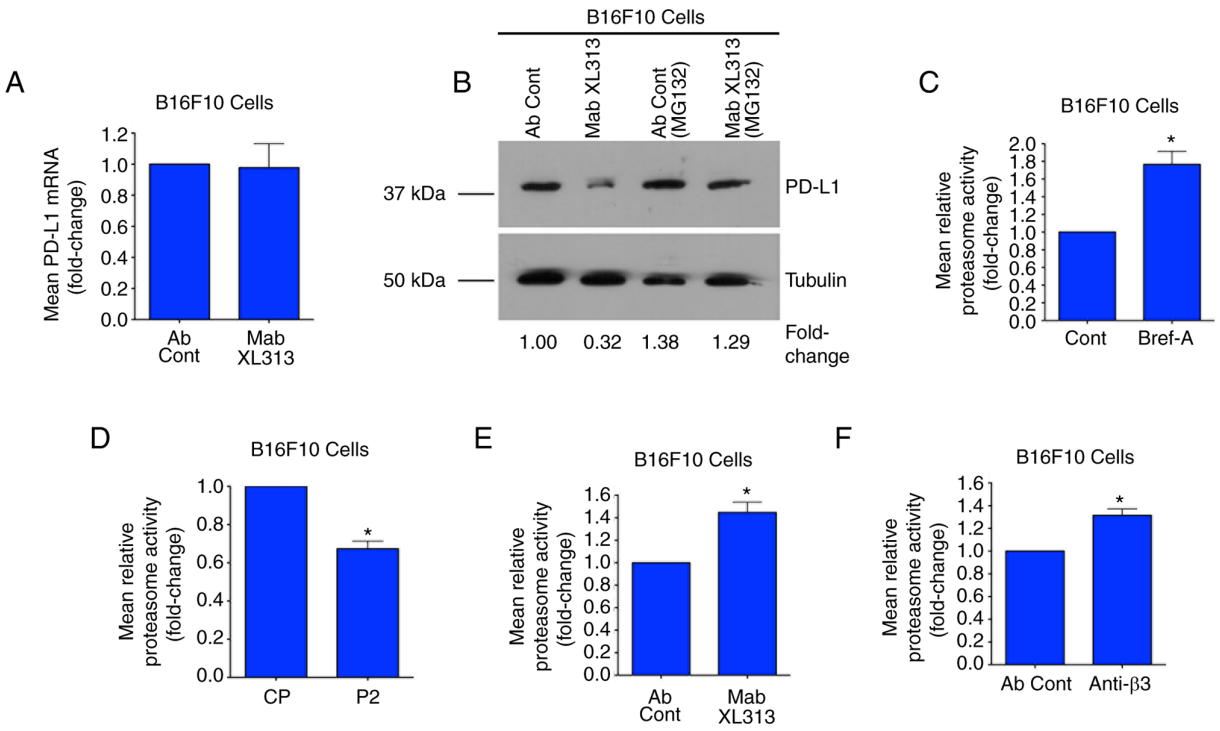

Figure 5. Reduction of PD-L1 levels in B16F10 cells by selectively targeting the RGDKGE collagen fragment is mediated by proteasome. (A) Quantification of the mean ± SEM fold change in PD-L1 mRNA levels in non-attached B16F10 cells treated for 15 min with non-specific control antibody (Ab Cont) or anti-RGDKGE collagen fragment antibody (Mab XL313) from 3 independent experiments. (B) Western blot analysis of whole cell lysates for PD-L1 or control tubulin in non-attached B16F10 cells pre-treated with either control buffer DMSO or the proteasome inhibitor MG132, then treated with anti-RGDKGE collagen fragment antibody (Mab XL313) or non-specific control (Ab Cont) for 15 min. (C and D) Quantification of the mean ± SEM fold from 4 independent experiments change in the relative levels of proteasome activity in B16F10 cells (C) treated with either vehicle control or Bref-A and (D) treated with control peptide CP or the RGDKGE-containing collagen peptide P2. (E) Quantification of the mean ± SEM fold change in the relative levels of proteasome activity in B16F10 cells treated with either anti-RGDKGE collagen fragment antibody (Mab XL313) or non-specific control (Ab Cont) from 3 independent experiments. (F) Quantification of the mean ± SEM fold change in the levels of proteasome activity in B16F10 cells treated with anti-β3 integrin antibody (Anti-β3) or non-specific control (Ab Cont) from 3 independent experiments. *P<0.05. PD-L1, programmed death-ligand 1; Bref-A, Brefeldin-A.

and YAP (47,48), prompted the authors to examine whether PKA plays a role in the ability of the RGDKGE-containing collagen fragment to control PD-L1 in our model. First, it was examined whether YAP may affect the PKA activity. As revealed in Fig. 6A, the levels of PKA activity were elevated in cells in which YAP was knocked down. Since the RGDKGE-containing collagen fragment can control YAP nuclear localization, the impact this collagen peptide had on PKA activity was assessed. As shown in Fig. 6B, stimulation of B16F10 cells with exogenously added RGDKGE collagen peptide P2, reduced the levels of PKA activity compared with control peptide CP. Taking into consideration these results, it was sought to determine whether the ability of Mab XL313 to control the levels of PD-L1 may depend on PKA. Treatment of B16F10 cells with Mab XL313 enhanced the relative levels of PKA activity compared with control antibody-treated cells (Fig. 6C). In similar experiments, a function blocking antibody directed to β3 integrin, a receptor for the RGDKGE collagen fragment, also enhanced the relative levels of PKA activity in B16F10 cells (Fig. 6D).

Finally, it was sought to determine whether the ability of Mab XL313 to reduce PD-L1 depended on PKA by carrying out experiments in the presence or absence of PKA inhibitor H89. As demonstrated in Fig. 6E, while treatment of B16F10 cells with Mab XL313 under control (DMSO)-treated conditions reduced the levels of PD-L1, similar experiments performed with cells pre-treated with the PKA inhibitor failed to demonstrate significantly altered PD-L1 levels (Fig. 6E). Similar studies were carried out with a second PKA inhibitor (KT5720) which demonstrated similar results (Fig. S6A). Moreover, blocking PKA activity also prevented the ability of Mab XL313 to alter PD-L1 in C32 and YUMM1.7 cells (Fig. S6B and C, respectively). Collectively, these novel findings are consistent with a role for the RGDKGE-containing collagen fragment in controlling PD-L1 by a mechanism that involves PKA.

The in vivo inhibitory activity of Mab XL313 depends on levels of tumor-associated PD-L1. The functional role of integrin-mediated signaling in controlling angiogenesis and tumor growth is well established (49-52). However, while the overall therapeutic strategy of directly targeting integrins such as αvβ3 to control tumor growth has shown activity in animal models and in human clinical studies (49-52), the overall impact of this approach has been limited (52). Among some of the possible reasons for the modest therapeutic benefit include the complexity of the cellular processes controlled by integrins such as αvβ3, which include both pro-tumorigenic and anti-tumorigenic signaling (53-58). Importantly, the ability of integrin signaling to control tumors depends on the functional contributions of the distinct cell types that express the integrin and the nature of the signaling pathways disrupted by directly

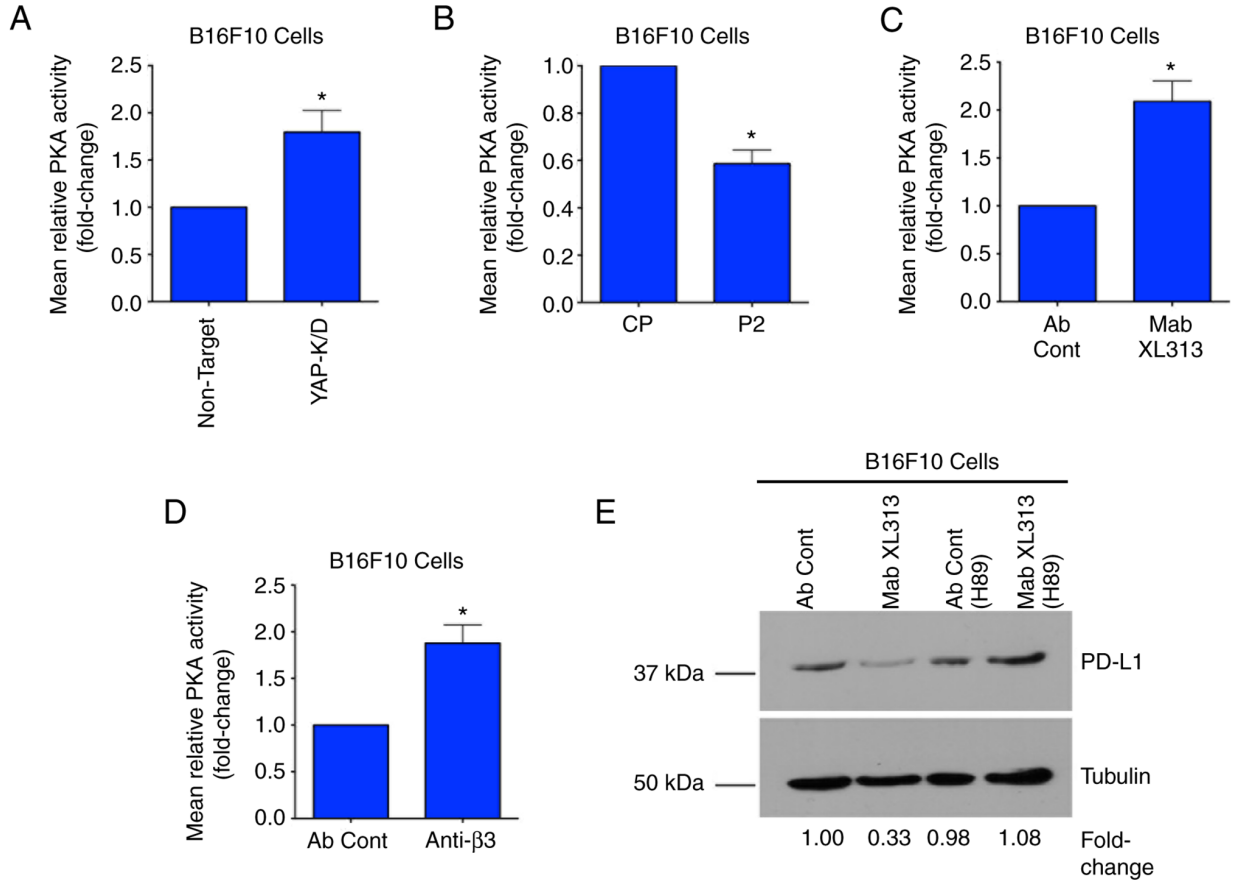

Figure 6. Reduction of PD-L1 levels in B16F10 cells by selectively targeting the RGDKGE collagen fragment depends on PKA activity. (A) Quantification of the mean ± SEM fold change in the relative levels of PKA activity in non-attached control-transfected B16F10 cells (B16F10-NT) or *Yap*-shRNA knock down B16F10 cells (B16F10-YAP/K/D) from 3 independent experiments. (B) Quantification of the mean ± SEM fold change in the relative levels of PKA activity in non-attached B16F10 cells treated with non-specific control peptide CP or RGDKGE-containing collagen peptide P2 for 15 min from 3 independent experiments. (C) Quantification of the mean ± SEM fold change in the relative levels of PKA activity in non-attached B16F10 cells treated with non-specific control antibody (Ab Cont) or anti-RGDKGE collagen fragment antibody (Mab XL313) for 15 min from 3 independent experiments. (D) Quantification of the mean ± SEM fold change in the relative levels of PKA activity in non-attached B16F10 cells treated with either non-specific control antibody (Ab Cont) or anti-β3 integrin antibody (Anti-β3) for 15 min from 3 independent experiments. (E) Western blot analysis of whole cell lysates for PD-L1 or control tubulin in non-attached B16F10 cells pre-treated with either control buffer DMSO or the PKA inhibitor H89, then treated with anti-RGDKGE collagen fragment antibody (Mab XL313) or non-specific control (Ab Cont) for 15 min. *P<0.05. PD-L1, programmed death-ligand 1; PKA, protein kinase-A; Mab, monoclonal antibody.

targeting the integrins. Thus, a therapeutic strategy that selectively targets a pro-tumorigenic ligand of the integrin rather than the integrin receptor itself, may provide a therapeutically effective alternative strategy.

Taking into consideration the present studies indicating that disrupting cellular interactions with the secreted RGDKGE-containing collagen fragment could reduce PD-L1 and inhibit tumor growth, it was sought to determine whether the antitumor activity of Mab XL313 depended on the levels of PD-L1. To this end, the antitumor effects of Mab XL313 on the growth of B16F10 tumors that had reduced levels of PD-L1 were examined (Fig. S7). As revealed in Fig. 7A and B and Table SIII, Mab XL313 inhibited the growth of control-transfected B16F10 tumors. By contrast, treatment of mice with Mab XL313 failed to significantly alter B16F10 tumor growth in which PD-L1 was knocked down (Fig. 7C and D and Table SIV). These findings are consistent with the capacity of Mab XL313 to inhibit tumor growth that depends on levels of PD-L1. Taken together, the present studies are consistent with a working model by which selectively targeting the secreted RGDKGE-containing collagen fragment prevents it from binding and signaling through integrin β3, thereby reducing the levels of nuclear localized YAP and enhancing PKA activity, which ultimately contributes to the reduction of PD-L1 by controlling its proteasomal-mediated degradation (Fig. 7E).

Discussion

It has been suggested that alterations in collagen density, fiber orientation as well as its molecular architecture correlates with phenotypic changes in different malignant tumors (59-63). In fact, second harmonic generation imaging of tumor biopsies has revealed unique collagen organizational signatures between normal tissues and tumors (59-63). Biophysical alterations in collagen structure can alter signaling that controls cell adhesion, migration and proliferation, and selective targeting of certain cryptic collagen elements can inhibit angiogenesis, tumor growth and metastasis in animal models (3,9,10,31,64). These and other findings not only implicate collagen as an important regulator of malignant tumors, but also suggests that discrete changes in its geometrical configuration play

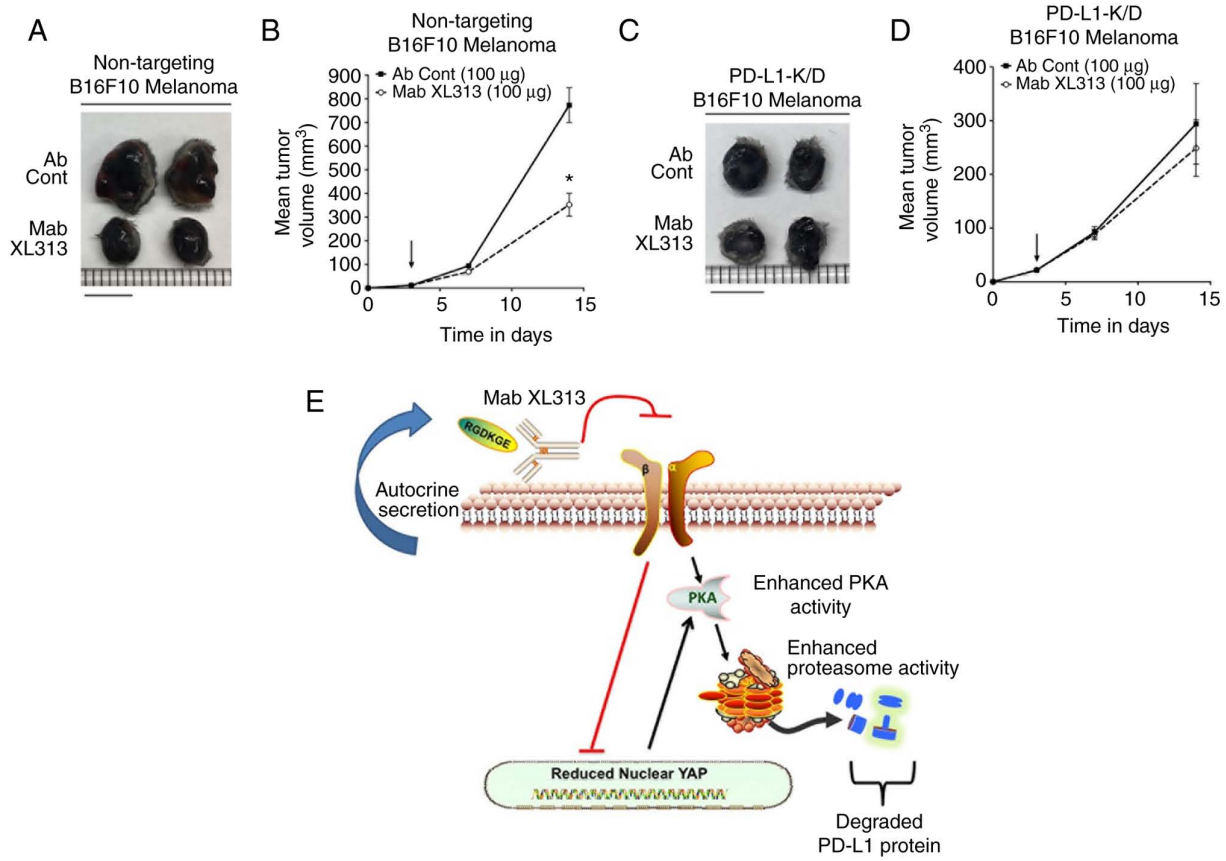

Figure 7. Inhibition of B16F10 tumor growth by Mab XL313 depends on PD-L1 levels. (A) Example of changes in control non-targeting B16F10 tumor size following treatment of mice with Mab XL313 or control antibody (Ab Cont) (scale bar, 1 cm). (B) Quantification of the effects of anti-RGDKGE collagen fragment antibody (Mab XL313) or non-specific control antibody (Ab Cont) on the growth of control non-targeting transfected B16F10 tumor cells (Non-Targeting-B16F10). Arrow indicates start of treatment with antibodies. Data points indicate the mean ± SEM tumor volumes (n=10-11 per group). P-value indicates comparison to control at each time point. (C) Example of changes in PD-L1-K/D B16F10 tumor size following treatment of mice with Mab XL313 or control antibody (Ab Cont), (scale bar, 1 cm). (D) Quantification of the effects of anti-RGDKGE collagen fragment antibody (Mab XL313) or non-specific control antibody (Ab Cont) on the growth of B16F10 tumor cells in which PD-L1 levels have been knocked down (PD-L1-K/D B16F10). Arrow indicates start of treatment with antibodies. Data points indicate the mean ± SEM tumor volumes (n=10 per group). (E) Working model of a potential mechanism by which selectively targeting the endogenously generated RGDKGE collagen fragment may regulate PD-L1 levels. Blocking the secreted RGDKGE-containing collagen fragment with anti-XL313 Mab inhibits this collagen fragment from binding and signaling through integrin β3, thereby reducing the levels of nuclear YAP and enhancing PKA activity, which contributes to the reduction of PD-L1 by enhancing proteasomal-mediated degradation. *P<0.05 vs. control at each time point. PD-L1, programmed death-ligand 1; Mab, monoclonal antibody; PKA, protein kinase-A.

distinct roles in stimulating signaling cascades that control tumor progression.

In addition to alterations in the biophysical features of insoluble collagen fibers, evidence suggested that certain circulating fragments of collagen correlate with aggressive behavior of a variety of histologically different tumor types, including, colon, breast and pancreatic carcinomas, as well as melanomas (65-68). High levels of circulating collagen fragments not only correlate with more aggressive disease, but also correlate with poor clinical outcomes following therapeutic intervention (65-68). For example, studies have correlated poor clinical responses in humans treated with immune checkpoint inhibitors targeting CTLA-4 and PD-1/PD-L1, with high levels of circulating collagen fragments (14,15). While these studies provided evidence of the differential levels of soluble collagen peptides during tumor progression and treatment, little evidence is available as to whether these fragments play direct functional roles in controlling tumor growth. Evidence suggested that soluble collagen-derived fragments may not only represent useful biomarkers, but may also have biological activity. In this regard, an MMP-2 generated proteolytic fragment of the a1chain of collagen type-I (C-1158/59) has been detected in human plasma and a synthetic peptide corresponding to this fragment demonstrated the ability to alter fibroblast migration, angiogenesis, fibrosis, wound healing, and ventricle dilation (69). Moreover endotrophin, a bioactive fragment of the a3 chain of collagen type-VI, modulates recruitment of macrophages and endothelial cells and regulates angiogenesis and tumor growth *in vivo* (70). These and other studies suggested that soluble collagen fragments indeed play roles in regulating tumor growth *in vivo*.

Our laboratory identified an RGDKGE-containing collagen peptide that was initially discovered as an endogenously secreted bioactive collagen fragment from M2-like macrophages (9). This collagen fragment was shown to regulate nuclear accumulation of YAP in endothelial cells and control cytokine-induced angiogenesis *in vivo* (9). The expression of this collagen fragment was not simply restricted to activated M2-like macrophages, but could also be expressed by tumors such as ovarian carcinomas (10). In fact, this collagen peptide

was capable of regulating nuclear accumulation of YAP in ovarian carcinoma cells by a mechanism associated with modulating the phosphorylation of the hippo effector kinase LATS1 (10). Selectively blocking binding of the RGDKGE collagen fragment led to enhanced LATS1 phosphorylation, and increased phosphorylation of YAP, which ultimately reduced the levels of nuclear YAP, and inhibited ovarian tumor growth *in vivo* (10).

While YAP is considered to regulate cell growth, it can also differentially control cell migration by modulating cytoskeletal dynamics as well as the expression and activity of small GTPases including ARHGAP29 (71-73). In certain cell types, YAP can also control the expression of the immune checkpoint molecule PD-L1 (11-13). While evidence indicated that targeting PD-L1 can help to control the growth of a variety of different tumor types, only a fraction of subjects treated with current anti-PD-L1 antagonists show significant and durable responses (14-17,19,20,39). Thus, it is important to develop a more in-depth understanding of the various mechanisms by which the levels of PD-L1 are controlled, as well as the unique functional impact of this immune checkpoint molecule has in different cell types. Recent evidence continues to provide new understanding of the complicated roles played by PD-L1 during tumor growth. For example, beyond the well characterized effects of PD-L1 in regulating immune evasion through binding to PD-1, studies have also uncovered evidence for tumor cell intrinsic signaling by PD-L1, thereby helping to control multiple processes such as regulating gene expression, proliferation, apoptosis and cell cycle control (74-77). In addition to cell surface expression of PD-L1, the release of soluble forms of PD-L1 can also contribute to regulating growth of tumors (78). Moreover, a recent study revealed that differential sub-cellular localization of PD-L1 in the nucleus of certain cell types, may help actively control cell survival and apoptosis (79). Given the diversity of functions of cell-associated and soluble forms of PD-L1, uncovering new mechanisms by which PD-L1 expression can be controlled may help in designing new strategies to limit therapeutic resistance and enhance the antitumor activity of immune checkpoint inhibition.

In this regard, unique mechanisms by which PD-L1 can be regulated continue to be uncovered as investigators have provided evidence for the ability of *Fusobacterium nucleatum* to regulate PD-L1 in colorectal cancer (80). In addition, a recent study also demonstrated a novel pathway by which RNA-RNA cross-talk can function in-conjunction with RICTOR to control PD-L1 expressing exosomes that affect hepatocellular carcinoma tumor growth (81). In further studies, metformin has been shown to help control PD-L1 levels by a unique mechanism involving ERAD-associated proteasome-mediated degradation of this immune checkpoint molecule (23). Notably, recent studies have also shown that metformin can affect YAP which is also known to regulate PD-L1 (23,82). In fact, the ability of metformin to control PD-L1 in some cell types may depend at least in part, on the activation of the Hippo signaling leading to enhanced phosphorylation of YAP and reduced levels of nuclear YAP (82). These studies provided additional understanding of the complicated roles played by YAP in its ability to control both PD-L1 expression as well as tumor growth.

Adding to the complexity by which YAP controls cellular behavior, YAP may exhibit opposing functions on tumor growth depending on the cell type it is functioning in. While enhanced YAP activity has been shown to promote the growth of several tumor types such as ovarian carcinomas and melanomas, other studies have implicated YAP in suppressing breast and liver cancers (10,11,31,83,84). These seemingly contradictory findings may be explained at least in part, by the differential roles that YAP plays in different cell types, as well as the different functional contributions of each unique cell type has on tumor growth. While YAP has been shown to play a role in regulating cytoskeletal dynamics required for efficient tumor cell motility (71,73) it may have the opposite effects in certain immune cell subsets (85,86). In this regard, reducing YAP activity can inhibit tumor growth and reduce T-Reg infiltration of tumors, while by contrast, blocking YAP activity may enhance $CD8^+$ T-cell motility and tumor infiltration (85-87). Moreover, previous studies have also demonstrated a role for YAP in regulating the pro-tumorigenic effects of macrophages as well as promoting the secretion of chemotactic factors that help recruit myeloid-derived suppressor cells (88-90). Therefore, a more in-depth analysis of the differential roles of YAP within distinct cellular compartments that control tumor growth is of critical importance as it relates to developing novel YAP based therapeutic strategies for the treatment of cancer (91).

In the present study, evidence was provided that the RGDKGE-containing cryptic collagen fragment can be secreted in a soluble form by an ER/Golgi-dependent mechanism. Additionally, this secreted collagen fragment can bind to β3 integrin in melanoma cells in an autocrine-like manner. Selectively targeting this collagen fragment can regulate nuclear accumulation of YAP that is independent from mechanisms associated with cell adhesion and spreading, as Mab XL313 treatment reduced nuclear YAP levels in melanoma cells held in suspension. These observations are consistent with previous studies indicating that YAP activation and its nuclear accumulation can occur by multiple mechanisms, including adhesion independent pathways (78).

As aforementioned, both YAP as well as integrin signaling has been implicated in regulating the levels of the immune-checkpoint molecule PD-L1. The present studies suggested for the first time, to the best of our knowledge, that specifically targeting the RGDKGE collagen fragment can lead to a reduction in the levels of PD-L1. The reduction in PD-L1 observed following treatment with Mab XL313 depended on YAP, as Mab XL313 failed to reduce PD-L1 in cells in which YAP was knocked down. Moreover, targeting β3 integrin with a function blocking antibody also reduced PD-L1 levels. These observations are consistent with the concept that blocking binding of this collagen peptide to β3 integrin results in suppressing an autocrine-like signaling cascade that controls PD-L1 levels. While studies have implicated β3 integrin signaling in regulating PD-L1 gene expression (29), the ability of Mab XL313 to reduce PD-L1 levels was not associated with significant changes in PD-L1 mRNA.

Notably, while targeting the secreted RGDKGE collagen fragment with Mab XL313 inhibited PD-L1 levels, Mab Xl313 failed to significantly reduce PD-L1 in cells pre-treated with the proteasome inhibitor, indicating that the ability of Mab

XL313 to reduce PD-L1 in these cells required proteasome activity. The proteasome functions as a major regulator of signaling cascades by rapidly controlling the levels of effector molecules (92). For example, cell attachment to the ECM protein fibronectin induced alterations in the small GTPases Rac and CDC42, ultimately leading to enhance proteasome activity and enhanced degradation of the cyclin dependent kinase $P21^{CIP1}$ (93). Notably, members of both the β1 and β3 integrin subfamilies can bind to fibronectin and mediate downstream signaling from this ECM molecule. These studies are consistent with the possibility that integrin-mediated signaling can differentially affect proteasome function. Consistent with this notion, treatment of neuroblastoma cells with a β1 integrin binding fibronectin peptide resulted in inactivation of β1 integrin, which enhanced proteasome dependent degradation of Myc proteins (94). These observations are similar to the present studies, in which the selective blockade of the RGDKGE-containing collagen peptide binding to β3 integrin resulted in enhanced proteasome-mediated degradation of PD-L1.

While the relative levels of cellular proteasome activity can be affected by multiple mechanisms, notably, previous studies have implicated PKA in regulating proteasome activity (41-44). Integrin signaling can differentially regulate PKA activity (45,46) and play roles in regulating YAP activity, angiogenesis, tumor growth and metastasis (47,48). Given the ability of Mab XL313 to reduce the levels of nuclear YAP, it was examined whether reducing YAP may affect the levels of PKA activity. The findings of the present study suggested that reducing the levels of YAP can enhance PKA activity in B16F10 cells. Moreover, stimulation with the synthetic RGDKGE-containing collagen peptide (P2) reduced PKA activity, while direct targeting of this collagen fragment or its cell surface receptor β3 integrin, enhanced PKA activity. Currently, the exact molecular mechanism by which the RGDKGE collagen fragment functions through β3 integrin to control PKA activity, and how YAP and PKA contributes to the control of proteasome activity are not completely understood. To this end, it would be interesting in the future to make use of FRET-based PKA sensors to study how the RGDKGE collagen fragment may function through β3 integrin in cells to regulate PKA and proteasome activity in order to define this signaling pathway in more detail.

Direct targeting of β3 integrin has demonstrated antitumor activity in animal models as well as in human subjects, however the overall therapeutic activity was limited. Among the possible explanations for this limited antitumor activity, the complex and opposing roles played by β3 integrin in distinct stromal cell compartments are included (50-53). The opposing roles played by different stromal cell types on tumor progression have been illustrated by studies focusing on the impact of differentially polarized stromal cells on tumor growth. For example, in the case of cancer associated fibroblast (CAFs), conflicting outcomes using a strategy to target CAFs to inhibit tumor growth have been observed, as depleting fibroblast activation protein expressing fibroblasts resulted in reduced tumor growth in pancreatic cancer, while depletion of αSMA-expressing fibroblasts resulted in more aggressive disease (95,96). In addition, macrophages can also have opposing roles in tumor progression, as demonstrated by the fact that while M1-like macrophages help eliminate tumor cells, M2-like macrophage, as well as myeloid-derived suppressor cells, are considered to promote tumor growth (57,58,89). Finally, while infiltration of $CD8^+$ cytotoxic T-cells play roles in inhibiting tumor growth, regulatory T-cells can help facilitate tumor progression (85-87). Given the fact that these stromal cell types may differentially express integrins including β3 integrin (85-90,92,93), a clinical strategy that seeks to directly target the global function of β3 integrin in all cell types including stromal cells such as M1-like macrophages and $CD8^+$ effector T-cells, may result in suboptimal clinical outcomes, and actually limit the overall effectiveness of this therapeutic strategy. Developing novel approaches to control β3 integrin signaling within the pro-tumorigenic cellular compartments without directly targeting β3 integrin itself, may allow for a new alternative approach to selectively control pro-tumorigenic signaling from β3 integrin without disrupting its anti-tumorigenic activity (57,58,97,98).

While our previous studies have shown that anti-XL313 antibody can inhibit the growth of ovarian tumors, which was associated with altered regulation of nuclear YAP, the ability of YAP to affect the growth of different types of tumor can vary considerably (10,11,31,83,84). In the present study, previous studies by the authors were extended and several new experimental findings that substantially improve our current understanding of how the RGDKGE collagen fragment may function were provided. First, it was demonstrated that the ability of the anti-XL313 Mab to inhibit tumor growth is not restricted to ovarian tumors, but can also affect the growth of other tumor types such as melanoma and mammary carcinomas *in vivo*. In addition, it was revealed that the RGDKGE collagen fragment can be generated inside cells by a cathepsin-associated mechanism and can be released extracellularly in a soluble form by an ER/Golgi dependent process. Moreover, evidence was provided for the first time, for a previously unappreciated ability of the RGDKGE collagen fragment to function in an autocrine-like manner to regulate the levels of PD-L1 by a PKA and proteasome-dependent mechanism. Collectively, these novel findings provided important new insight into the roles by which the soluble RGDKGE collagen fragment may affect tumor growth.

In summary, new evidence was provided that selectively targeting a secreted pro-tumorigenic ligand of β3 integrin, instead of directly targeting β3 integrin itself, can inhibit B16F10 and 4T1 tumor growth *in vivo*. While Mab XL313 significantly inhibited control transfected B16F10 tumors, this antibody failed to inhibit the growth of B16F10 tumors in which PDL-1 was knocked down, indicating an important role for PD-L1 in the ability of the RGDKGE collagen fragment to control B16F10 tumor growth *in vivo*. Taken together, our studies provided evidence for an autocrine-like signaling pathway involving β3 integrin that provides tumor cells with the ability to regulate proteasome-mediated control of PD-L1 by modulating the activity of PKA and YAP. Moreover, our new findings may help in establishing a selective new alternative strategy to control pro-tumorigenic activity of β3-integrin signaling without directly disrupting β3 integrin's tumor suppressing functions in other cell populations.

Acknowledgements

Not applicable.

Funding

The present study was supported in part from NIH (grant no. CA196739). Further support was from the Northern New England Clinical and Translational Research Center (CTR; grant no. U54GM115516), and the Mesenchymal and Neural Regulation of Metabolic Networks (grant no. P20GM121301. Partial support was also provided by NIH (grant nos. RO1 CA238237, U54 CA224070 and PO1 CA114046) and the Dr. Miriam and Sheldon G. Adelson Medical Research Foundation. Additional support was provided by the Maine Medical Center and the Cross Insurance Agency, John Benoit and Thomas Holden.

Availability of data and materials

The datasets used and/or analyzed during the current study are available from the corresponding author on reasonable request.

Authors' contributions

JMC helped conceive, design, coordinate studies, performed and analyzed experiments and helped write, review and edited the manuscript. XH helped conceive, design, coordinate studies, performed and analyze experiments and helped write, review and edited the manuscript. CWL, PS, SCR and MSE assisted in analysis and interpretation of the data and writing, reviewing and editing the manuscript. MH helped coordinate studies, assisted in analysis and interpretation of the data and in writing, reviewing and editing of the manuscript. PCB helped conceive, design, coordinate studies, analyzed experiments, and interpreted the data, and helped write, review and edited the manuscript. All authors read and approved the final version of the manuscript and agree to be accountable for all aspects of the work. JMC, XH and PCB confirm the authenticity of the raw data.

Ethics approval and consent to participate

Anonymous de-identified human tumor samples were used. Use of the human tumor samples were considered exempt as it relates to human subjects' research by MaineHealth IRB and Biobank as all tissues were anonymous and de-identified. Animal studies were approved by the Maine Medical Center Institutional Animal Care and Use Committee (Scarborough, USA).

Patient consent for publication

Not applicable.

Competing interests

PCB holds an equity position in CryptoMedix, Inc. The rest of the authors declare that they have no competing interests.

References

1. Brassart-Pasco S, Brezillon S, Brassart B, Ramont L, Oudart JB and Monboisse JC: Tumor microenvironment: Extracellular matrix alterations influence tumor progression. Front Oncol 10: 397, 2020.
2. Ruiter D, Bogenrieder T, Elder D and Herlyn M: Melanoma-stroma interactions: Structural and functional aspects. Lancet Oncol 3: 35-43, 2002.
3. Han X, Caron JM and Brooks PC: Cryptic collagen elements as signaling hubs in the regulation of tumor growth and metastasis. J Cell Physiol 235: 9005-9020, 2020.
4. Contois L, Akalu A and Brooks PC: Integrins as 'functional hubs' in the regulation of pathological angiogenesis. Semin Cancer Biol 19: 318-328, 2009.
5. Ricard-Blum S: The collagen family. Cold Spring Harb Perspect Biol 3: a004978, 2011.
6. Zeltz C and Gullberg D: The integrin-collagen connection-a glue for tissue repair? J Cell Sci 129: 1284, 2016.
7. Leitinger B: Transmembrane collagen receptors. Annu Rev Cell Dev Biol 27: 265-290, 2011.
8. Bienkowski RS, Curran SF and Berg RA: Kinetics of intracellular degradation of newly synthesized collagen. Biochemistry 25: 2455-2459, 1986.
9. Ames JJ, Contois L, Caron JM, Tweedie E, Yang X, Friesel R, Vary C and Brooks PC: Identification of an endogenously generated cryptic collagen epitope (XL313) that may selectively regulate angiogenesis by an integrin yes-associated protein (YAP) mechano-transduction pathway. J Biol Chem 291: 2731-2750, 2016.
10. Han X, Caron JM, Lary CW, Sathyanarayana P, Vary C and Brooks PC: An RGDKGE-containing cryptic collagen fragment regulates phosphorylation of large tumor suppressor kinase-1 and controls ovarian tumor growth by a YAP-associated protein-dependent mechanism. Am J Pathol 191: 527-544, 2021.
11. Kim MH, Kim CG, Kim SK, Shin SJ, Choe EA, Park SH, Shin EC and Kim J: YAP-induced PD-L1 expression drives immune evasion in BRAFi-resistant melanoma. Cancer Immunol Res 6: 255-266, 2018.
12. Hsu PC, Miao J, Wang YC, Zhang WQ, Yang YL, Wang CW, Yang CT, Huang Z, You J, Xu Z, *et al*: Inhibition of yes-associated protein down-regulates PD-L1 (CD274) expression in human malignant pleural mesothelioma. J Cell Mol Med 22: 3139-3148, 2018.
13. Lee BS, Park DI, Lee DH, Lee JE, Yeo MK, Park YH, Lim DS, Choi W, Lee DH, Yoo G, *et al*: Hippo effector YAP directly regulates the expression of PD-L1 transcripts in EGFR-TKI-resistant lung adenocarcinoma. Biochem Biophy Res Commun 491: 493-499, 2017.
14. Jensen C, Madsen DH, Hansen M, Schmidt H, Svane IM, Karsdal MA and Willumsen N: Non-invasive biomarkers derived from the extracellular matrix associate with response to immune checkpoint blockade (anti-CTLA-4) in metastatic melanoma patients. J Immunother Cancer 6: 152, 2018.
15. Hurkmans DP, Jensen C, Koolen SLW, Aerts J, Karsdal MA, Mathijssen RHJ and Willumsen N: Blood-based extracellular matrix biomarkers are correlated with clinical outcome after PD-1 inhibition in patients with metastatic melanoma. J Immunother Cancer 8: e001193, 2020.
16. Abdou Y, Pandey M, Sarma M, Shah S, Baron J and Ernstoff MS: Mechanism-based treatment of cancer with immune checkpoint inhibitor therapies. Br J Clin Pharmacol 86: 1690-1702, 2020.
17. Gandhi S, Pandey MR, Attwood K, Ji W, Witkiewicz AK, Knudsen ES, Allen C, Tario JD, Wallace PK, Cedeno CD, *et al*: Phase I clinical trial of combination propranolol and pembrolizumab in locally advanced and metastatic melanoma: Safety, tolerability, and preliminary evidence of antitumor activity. Clin Cancer Res 27: 87-95, 2021.
18. Somasundaram R, Connelly T, Choi R, Choi H, Samarkina A, Li L, Gregorio E, Chen Y, Thakur R, Abdel-Mohsen M, *et al*: Tumor-infiltrating mast cells are associated with resistance to anti-PD-1 therapy. Nat Commun 12: 346, 2021.
19. Cha JH, Chan LC, Li CW, Hsu JL and Hung MC: Mechanisms controlling PD-L1 expression in cancer. Mol Cell 76: 359-370, 2019.
20. Sun C, Mezzadra R and Schumacher TN: Regulation and function of the PD-L1 checkpoint. Immunity 48: 434-452, 2018.
21. Gou Q, Dong C, Xu H, Khan B, Jin J, Liu Q, Shi J and Hou Y: PD-L1 degradation pathway and immunotherapy for cancer. Cell Death Dis 11: 955, 2020.

22. Li CW, Lim SO, Xia W, Lee HH, Chan LC, Kuo CW, Khoo KH, Chang SS, Cha JH, Kim T, *et al*: Glycosylation and stabilization of programmed death ligand-1 suppresses T-cell activity. Nat Commun 7: 12632, 2016.
23. Cha JH, Yang WH, Xia W, Wei Y, Chan LC, Lim SO, Li CW, Kim T, Chang SS, Lee HH, *et al*: Metformin promotes antitumor immunity via endoplasmic-reticulum-associated degradation of PD-L1. Mol Cell 71: 606-620.e7, 2018.
24. Burr ML, Sparbier CE, Chan YC, Williamson JC, Woods K, Beavis PA, Lam EYN, Henderson MA, Bell CC, Stolzenburg S, *et al*: CMTM6 maintains the expression of PD-L1 and regulates anti-tumour immunity. Nature 549: 101-105, 2017.
25. Wang H, Yao H, Li C, Shi H, Lan J, Li Z, Zhang Y, Liang L, Fang JY and Xu J: HIP1R targets PD-L1 to lysosomal degradation to alter T cell-mediated cytotoxicity. Nat Chem Biol 15: 42-50, 2019.
26. Coelho MA, de Carné Trécesson S, Rana S, Zecchin D, Moore C, Molina-Arcas M, East P, Spencer-Dene B, Nye E, Barnouin K, *et al*: Oncogenic RAS signaling promotes tumor immunoresistance by stabilizing PD-L1 mRNA. Immunity 47: 1083-1099.e6, 2017.
27. Lin HY, Chin YT, Nana AW, Shih YJ, Lai HY, Tang HY, Leinung M, Mousa SA and Davis PJ: Actions of l-thyroxine and Nano-diamino-tetrac (Nanotetrac) on PD-L1 in cancer cells. Steroids 114: 59-67, 2016.
28. Ren D, Zhao J, Sun Y, Li D, Meng Z, Wang B, Fan P, Liu Z, Jin X and Wu H: Overexpressed ITGA2 promotes malignant tumor aggression by up-regulating PD-L1 expression through the activation of the STAT3 signaling pathway. J Exp Clin Cancer Res 38: 485, 2019.
29. Vannini A, Leoni V, Barboni C, Sanapo M, Zaghini A, Malatesta P, Campadelli-Fiume G and Gianni T: αvβ3-integrin regulates PD-L1 expression and is involved in cancer immune evasion. Proc Natl Acad Sci USA 116: 20141-20150, 2019.
30. Livak KJ and Schmittgen TD: Analysis of relative gene expression data using real-time quantitative PCR and the 2(-Delta Delta C(T)) method. Methods 25: 402-408, 2001.
31. Caron JM, Han X, Contois L, Vary CPH and Brooks PC: The HU177 collagen epitope controls melanoma cell migration and experimental metastasis by a CDK5/YAP-dependent mechanism. Am J Pathol 188: 2356-2368, 2018.
32. Provenzano PP, Inman DR, Eliceiri KW, Knittel JG, Yan L, Rueden CT, White JG and Keely PJ: Collagen density promotes mammary tumor initiation and progression. BMC Med 6: 11, 2008.
33. Vellinga TT, den Uil S, Rinkes IH, Marvin D, Ponsioen B, Alvarez-Varela A, Fatrai S, Scheele C, Zwijnenburg DA, Snippert H, *et al*: Collagen-rich stroma in aggressive colon tumors induces mesenchymal gene expression and tumor cell invasion. Oncogene 35: 5263-5271, 2016.
34. van Kempen LC, Rijntjes J, Mamor-Cornelissen I, Vincent-Naulleau S, Gerritsen MJ, Ruiter DJ, van Dijk MC, Geffrotin C and van Muijen GN: Type I collagen expression contributes to angiogenesis and the development of deeply invasive cutaneous melanoma. Int J Cancer 122: 1019-1029, 2008.
35. Noel A, Munaut C, Boulvain A, Calberg-Bacq CM, Lambert CA, Nusgens B, Lapiere CM and Foidart JM: Modulation of collagen and fibronectin synthesis in fibroblasts by normal and malignant cells. J Cell Biochem 48: 150-161, 1992.
36. Afik R, Zigmond E, Vugman M, Klepfish M, Shimshoni E, Pasmanik-Chor M, Shenoy A, Bassat E, Halpern Z, Geiger T, *et al*: Tumor macrophages are pivotal constructors of tumor collagenous matrix. J Exp Med 213: 2315-2331, 2016.
37. Gupta HB, Clark CA, Yuan B, Sareddy G, Pandweswara S, Padron AS, Hurez V, Conejo-Garcia J, Vadlamudi R, Li R and Curiel TJ: Tumor cell-intrinsic PD-L1 promotes tumor-initiating cell generation and functions in melanoma and ovarian cancer. Signal Transduct Target Ther 1: 16030, 2016.
38. Clark CA, Gupta HB, Sareddy G, Pandeswara S, Lao S, Yuan B, Drerup JM, Padron A, Conejo-Garcia J, Murthy K, *et al*: Tumor-intrinsic PD-L1 signals regulate cell growth, pathogenesis, and autophagy in ovarian cancer and melanoma. Cancer Res 76: 6964-6974, 2016.
39. Hudson K, Cross N, Jordan-Mahy N and Leyland R: The extrinsic and intrinsic roles of PD-L1 and its receptor PD-1: Implications for immunotherapy treatment. Front Immunol 11: 568931, 2020.
40. Xue Z, Zheng S, Linghu D, Liu B, Yang Y, Chen MK, Huang H, Song J, Li H, Wang J, *et al*: PD-L1 deficiency sensitizes tumor cells to DNA-PK inhibition and enhances cGAS-STING activation. Am J Cancer Res 12: 2363-2375, 2022.
41. VerPlank JJS, Lokireddy S, Zhao J and Goldberg AL: 26S Proteasomes are rapidly activated by diverse hormones and physiological states that raise cAMP and cause Rpn6 phosphorylation. Proc Natl Acd Sci USA 116: 4228-4237, 2019.
42. Asai M, Tsukamoto O, Minamino T, Asanuma H, Fujita M, Asano Y, Takahama H, Sasaki H, Higo S, Asakura M, *et al*: PKA rapidly enhances proteasome assembly and activity in in vivo canine hearts. J Mol Cell Cardiol 46: 452-462, 2009.
43. Lokireddy S, Kukushkin NV and Goldberg AL: cAMP-induced phosphorylation of 26S proteasomes on Rpn6/PSMD11 enhances their activity and the degradation of misfolded proteins. Proc Natl Acad Sci USA 112: E7176-E7185, 2015.
44. Qin XY, Zhang YL, Chi YF, Yan B, Zeng XJ, Li HH and Liu Y: Angiotensin II regulates Th1 T cell differentiation through angiotensin II type 1 receptor-PKA-mediated activation of proteasome. Cell Physiol Biochem 45: 1366-1376, 2018.
45. Kim S, Harris M and Varner JA: Regulation of integrin alpha vbeta 3-mediated endothelial cell migration and angiogenesis by integrin alpha5beta1 and protein kinase A. J Biol Chem 275: 33920-33928, 2000.
46. Whelan MC and Senger DR: Collagen I initiates endothelial cell morphogenesis by inducing actin polymerization through suppression of cyclic AMP and protein kinase A. J Biol Chem 278: 327-334. 2003.
47. Kim M, Kim M, Lee S, Kuninaka S, Saya H, Lee H, Lee S and Lim DS: cAMP/PKA signalling reinforces the LATS-YAP pathway to fully suppress YAP in response to actin cytoskeletal changes. EMBO J 32: 1543-1555, 2013.
48. Yu FX, Zhang Y, Park HW, Jewell JL, Chen Q, Deng Y, Pan D, Taylor SS, Lai ZC and Guan KL: Protein kinase A activates the hippo pathway to modulate cell proliferation and differentiation. Genes Devel 27: 1223-1232, 2013.
49. Brooks PC, Clark RA and Cheresh DA: Requirement of vascular integrin alpha v beta 3 for angiogenesis. Science 264: 569-571, 1994.
50. Brooks PC, Montgomery AM, Rosenfeld M, Reisfeld RA, Hu T, Klier G and Cheresh DA: Integrin alpha v beta 3 antagonists promote tumor regression by inducing apoptosis of angiogenic blood vessels. Cell 79: 1157-1164, 1994.
51. Delbaldo C, Raymond E, Vera K, Hammershaimb L, Kaucic K, Lozahic S, Marty M and Faivre S: Phase I and pharmacokinetic study of etaracizumab (Abegrin), a humanized monoclonal antibody against alphαvβeta3 integrin receptor, in patients with advanced solid tumors. Invest New Drugs 26: 35-43, 2008.
52. Hersey P, Sosman J, O'Day S, Richards J, Bedikian A, Gonzalez R, Sharfman W, Weber R, Logan T, Buzoianu M, *et al*: A randomized phase 2 study of etaracizumab, a monoclonal antibody against integrin alpha(v)beta(3), + or -dacarbazine in patients with stage IV metastatic melanoma. Cancer 116: 1526-1534, 2010.
53. Petitclerc E, Strömblad S, von Schalscha TL, Mitjans F, Piulats J, Montgomery AM, Cheresh DA and Brooks PC: Integrin alpha(v) beta3 promotes M21 melanoma growth in human skin by regulating tumor cell survival. Cancer Res 59: 2724-2730, 1999.
54. Natali PG, Hamby CV, Felding-Habermann B, Liang B, Nicotra MR, Di Filippo F, Giannarelli D, Temponi M and Ferrone S: Clinical significance of alpha(v)beta3 integrin and intercellular adhesion molecule-1 expression in cutaneous malignant melanoma lesions. Cancer Res 57: 1554-1560, 1997.
55. Kanamori M, Vanden Berg SR, Bergers G, Berger MS and Pieper RO: Integrin beta3 overexpression suppresses tumor growth in a human model of gliomagenesis: Implications for the role of beta3 overexpression in glioblastoma multiforme. Cancer Res 64: 2751-2758, 2004.
56. Jinushi M, Chiba S, Baghdadi M, Kinoshita I, Dosaka-Akita H, Ito K, Yoshiyama H, Yagita H, Uede T and Takaoka A: ATM-mediated DNA damage signals mediate immune escape through integrin-αvβ3-dependent mechanisms. Cancer Res 72: 56-65, 2012.
57. Su X, Esser AK, Amend SR, Xiang J, Xu Y, Ross MH, Fox GC, Kobayashi T, Steri V, Roomp K, *et al*: Antagonizing integrin β3 increases immunosuppression in cancer. Cancer Res 76: 3484-3495, 2016.
58. Reynolds LE, Wyder L, Lively JC, Taverna D, Robinson SD, Huang X, Sheppard D, Hynes RO and Hodivala-Dilke KM: Enhanced pathological angiogenesis in mice lacking beta3 integrin or beta3 and beta5 integrins. Nature Med 8: 27-34, 2002.
59. Xi G, Guo W, Kang D, Ma J, Fu F, Qiu L, Zheng L, He J, Fang N, Chen J, *et al*: Large-scale tumor-associated collagen signatures identify high-risk breast cancer patients. Theranostics 11: 3229-3243, 2021.
60. Drifka CR, Loeffler AG, Mathewson K, Keikhosravi A, Eickhoff JC, Liu Y, Weber SM, Kao WJ and Eliceiri KW: Highly aligned stromal collagen is a negative prognostic factor following pancreatic ductal adenocarcinoma resection. Oncotarget 7: 76197-76213, 2016.

61. Wu PC, Hsieh TY, Tsai ZU and Liu TM: In vivo quantification of the structural changes of collagens in a melanoma microenvironment with second and third harmonic generation microscopy. Sci Rep 5: 8879, 2015.
62. Birk JW, Tadros M, Moezardalan K, Nadyarnykh O, Forouhar F, Anderson J and Campagnola P: Second harmonic generation imaging distinguishes both high-grade dysplasia and cancer from normal colonic mucosa. Dig Dis Sci 59: 1529-1534, 2014.
63. Burke K, Smid M, Dawes RP, Timmermans MA, Salzman P, van Deurzen CH, Beer DG, Foekens JA and Brown E: Using second harmonic generation to predict patient outcome in solid tumors. BMC Cancer 15: 929, 2015.
64. Xu J, Rodriguez D, Petitclerc E, Kim JJ, Hangai M, Moon YS, Davis GE and Brooks PC: Proteolytic exposure of a cryptic site within collagen type IV is required for angiogenesis and tumor growth in vivo. J Cell Biol 154: 1069-1079, 2001.
65. Willumsen N, Ali SM, Leitzel K, Drabick JJ, Yee N, Polimera HV, Nagabhairu V, Krecko L, Ali A, Maddukuri A, *et al*: Collagen fragments quantified in serum as measures of desmoplasia associate with survival outcome in patients with advanced pancreatic cancer. Sci Rep 9: 19761, 2019.
66. Kehlet SN, Sanz-Pamplona R, Brix S, Leeming DJ, Karsdal MA and Moreno V: Excessive collagen turnover products are released during colorectal cancer progression and elevated in serum from metastatic colorectal cancer patients. Sci Rep 6: 30599, 2016.
67. Lipton A, Leitzel K, Ali SM, Polimera HV, Nagabhairu V, Marks E, Richardson AE, Krecko L, Ali A, Koestler W, *et al*: High turnover of extracellular matrix reflected by specific protein fragments measured in serum is associated with poor outcomes in two metastatic breast cancer cohorts. Int J Cancer 143: 3027-3034, 2018.
68. Hamilton HK, Rose AE, Christos PJ, Shapiro RL, Berman RS, Mazumdar M, Ma MW, Krich D, Liebes L, Brooks PC and Osman I: Increased shedding of HU177 correlates with worse prognosis in primary melanoma. J Transl Med 8: 19, 2010.
69. Lindsey ML, Iyer RP, Zamilpa R, Yabluchanskiy A, DeLeon-Pennell KY, Hall ME, Kaplan A, Zouein FA, Bratton D, Flynn ER, *et al*: A novel collagen matricryptin reduces left ventricular dilation post-myocardial infarction by promoting scar formation and angiogenesis. J Am Coll Cardiol 66: 1364-1374, 2015.
70. Wang J and Pan W: The biological role of the collagen alpha-3 (VI) chain and its cleaved C5 domain fragment endotrophin in cancer. Onco Targets Ther 13: 5779-5793, 2020.
71. Jang JW, Kim MK and Bae SC: Reciprocal regulation of YAP/TAZ by the hippo pathway and the small GTPase pathway. Small GTPases 11: 280-288, 2020.
72. Feng X, Degese MS, Iglesias-Bartolome R, Vaque JP, Molinolo AA, Rodrigues M, Zaidi MR, Ksander BR, Merlino G, Sodhi A, *et al*: Hippo-independent activation of YAP by the GNAQ uveal melanoma oncogene through a trio-regulated rho GTPase signaling circuitry. Cancer Cell 25: 831-845, 2014.
73. Qiao Y, Chen J, Lim YB, Finch-Edmondson ML, Seshachalam VP, Qin L, Jiang T, Low BC, Singh H, Lim CT and Sudol M: YAP regulates actin dynamics through ARHGAP29 and promotes metastasis. Cell Rep 19: 1495-1502, 2017.
74. Kornepati AVR, Boyd JT, Murray CE, Saifetiarova J, de la Peña Avalos B, Rogers CM, Bai H, Padron AS, Liao Y, Ontiveros C, *et al*: Tumor intrinsic PD-L1 promotes DNA repair in distinct cancers and suppresses PARP inhibitor-induced synthetic lethality. Cancer Res 82: 2156-2170, 2022.
75. Lee JJ, Kim SY, Kim SH, Choi S, Lee B and Shin JS: STING mediates nuclear PD-L1 targeting-induced senescence in cancer cells. Cell Death Dis 13: 791. 2022.
76. Yu J, Qin B, Moyer AM, Nowsheen S, Tu X, Dong H, Boughey JC, Goetz MP, Weinshilboum R, Lou Z and Wang L: Regulation of sister chromatid cohesion by nuclear PD-L1. Cell Res 30: 590-601, 2020.
77. Ghebeh H, Lehe C, Barhoush E, Al-Romaih K, Tulbah A, Al-Alwan M, Hendrayani SF, Manogaran P, Alaiya A, Al-Tweigeri T, *et al*: Doxorubicin downregulates cell surface B7-H1 expression and upregulates its nuclear expression in breast cancer cells: Role of B7-H1 as an anti-apoptotic molecule. Breast Cancer Res 12: R48, 2010.
78. Ye L, Zhu Z, Chen X, Zhang H, Huang J, Gu S and Zhao X: The importance of exosomal PD-L1 in cancer progression and its potential as a therapeutic target. Cells 10: 3247, 2021.
79. Gao Y, Nihira NT, Bu X, Chu C, Zhang J, Kolodziejczyk A, Fan Y, Chan NT, Ma L, Liu J, *et al*: Acetylation-dependent regulation of PD-L1 nuclear translocation dictates the efficacy of anti-PD-1 immunotherapy. Nat Cell Biol 22: 1064-1075, 2020.
80. Gao Y, Bi D, Xie R, Li M, Gau J, Liu H, Guo X, Fang J, Ding T, Zhu H, *et al*: *Fusobacterium nucleatum* enhances the efficacy of PD-L1 blockade in colorectal cancer. Signal Transduct Target Ther 6: 398, 2021.
81. Wei Y, Tang X, Ren Y, Yang Y, Song F, Fu J, Liu S, Yi M, Chen J, Wang S, *et al*: An RNA-RNA crosstalk network involving HMGB1 and RICTOR facilitates hepatocellular carcinoma tumorigenesis by promoting glutamine metabolism and impedes immunotherapy by PD-L1+ exosomes activity. Signal Transduct Target Ther 6: 421, 2021.
82. Zhang JJ, Zhang QS, Li ZQ, Zhou JW and Du J: Metformin attenuates PD-L1 expression through activating hippo signaling pathway in colorectal cancer cells. Am J Transl Res 11: 6965-6976, 2019.
83. Moya IM, Castaldo SA, Van den Mooter L, Soheily S, Sansores-Garcia L, Jacobs J, Mannaerts I, Xie J, Verboven E, Hillen H, *et al*: Peritumoral activation of the hippo pathway effectors YAP and TAZ suppresses liver cancer in mice. Science 366: 1029-1034, 2019.
84. Yuan M, Tomlinson V, Lara R, Holliday D, Chelala C, Harada T, Gangeswaran R, Manson-Bishop C, Smith P, Danovi SA, *et al*: Yes-associated protein (YAP) functions as a tumor suppressor in breast. Cell Death Differ 15: 1752-1759, 2008.
85. Lebid A, Chung L, Pardoll DM and Pan F: YAP attenuates CD8 T cell-mediated anti-tumor response. Front Immunol 11: 580, 2020.
86. Stampouloglou E, Cheng N, Federico A, Slaby E, Monti S, Szeto GL and Varelas X: Yap suppresses T-cell function and infiltration in the tumor microenvironment. PLoS Biol 18: e3000591, 2020.
87. Ni X, Tao J, Barbi J, Chen Q, Park BV, Li Z, Zhang N, Lebid A, Ramaswamy A, Wei P, *et al*: YAP is essential for Treg-mediated suppression of antitumor immunity. Cancer Discov 8: 1026-1043, 2018.
88. Yang W, Yang S, Zhang F, Cheng F, Wang X and Rao J: Influence of the Hippo-YAP signalling pathway on tumor associated macrophages (TAMs) and its implications on cancer immunosuppressive microenvironment. Ann Transl Med 8: 399, 2020.
89. Wang G, Lu X, Dey P, Deng P, Wu CC, Jiang S, Fang Z, Zhao K, Konaparthi R, Hua S, *et al*: Targeting YAP-dependent MDSC infiltration impairs tumor progression. Cancer Discov 6: 80-95, 2016.
90. Shibata M, Ham K and Hoque MO: A time for YAP1: Tumorigenesis, immunosuppression and targeted therapy. Int J Cancer 143: 2133-2144, 2018.
91. Lee JY, Dominguez AA, Nam S, Stowers RS, Qi LS and Chaudhuri O: Identification of cell context-dependent YAP-associated proteins reveals β_1 and β_4 integrin mediate YAP translocation independently of cell spreading. Sci Rep 9: 17188, 2019.
92. Lecker SH, Goldberg AL and Mitch WE: Protein degradation by the ubiquitin-proteasome pathway in normal and disease states. J Am Soc Nephrol 17: 1807-1819, 2006.
93. Bao W, Thullberg M, Zhang H, Onischenko A and Strömblad S: Cell attachment to the extracellular matrix induces proteasomal degradation of p21(CIP1) via Cdc42/Rac1 signaling. Mol Cell Biol 22: 4587-4597, 2002.
94. Sasada M, Iyoda T, Asayama T, Suenaga Y, Sakai S, Kase N, Kodama H, Yokoi S, Isohama Y and Fukai F: Inactivation of beta1 integrin induces proteasomal degradation of Myc oncoproteins. Oncotarget 10: 4960-4972, 2019.
95. Kraman M, Bambrough PJ, Arnold JN, Roberts EW, Magiera L, Jones JO, Gopinathan A, Tuveson DA and Fearon DT: Suppression of antitumor immunity by stromal cells expressing fibroblast activation protein-alpha. Science 330: 827-830, 2010.
96. Özdemir BC, Pentcheva-Hoang T, Carstens JL, Zheng X, Wu CC, Simpson TR, Laklai H, Sugimoto H, Kahlert C, Novitskiy SV, *et al*: Depletion of carcinoma-associated fibroblasts and fibrosis induces immunosuppression and accelerates pancreas cancer with reduced survival. Cancer Cell 25: 719-734, 2014.
97. Legler DF, Johnson-Léger C, Wiedle G, Bron C and Imhof BA: The alpha v beta 3 integrin as a tumor homing ligand for lymphocytes. Eur J Immunol 34: 1608-1616, 2004.
98. Larochelle C, Uphaus T, Broux B, Gowing E, Paterka M, Michel L, Dudvarski Stankovic N, Bicker F, Lemaître F, Prat A, *et al*: EGFL7 reduces CNS inflammation in mouse. Nature Commun 9: 819, 2018.